

Cosmological simulations of the growth of supermassive black holes and feedback from active galactic nuclei: method and tests

C. M. Booth^{1*} and Joop Schaye¹

¹*Leiden Observatory, Leiden University, PO Box 9513, 2300 RA Leiden, the Netherlands*

26 October 2018

ABSTRACT

We present a method that self-consistently tracks the growth of supermassive black holes (BHs) and the feedback from active galactic nuclei (AGN) in cosmological, hydrodynamical simulations. Our model is a substantially modified version of the one introduced by Springel et al. (2005) implemented in a significantly expanded version of the GADGET III code, which contains new prescriptions for star formation, supernova feedback, radiative cooling and chemodynamics. We simulate the growth of BHs from an initial seed state via Eddington-limited accretion of the surrounding gas, and via mergers with other BHs. Because cosmological simulations at present lack both the resolution and the physics to model the multiphase interstellar medium, they tend to strongly underestimate the Bondi-Hoyle accretion rate. To allow low-mass BHs to grow, it is therefore necessary to increase the predicted Bondi-Hoyle rates in star-forming gas by large factors, either by explicitly multiplying the accretion rate by a numerical correction factor, or using an unresolved, subgrid model for the gas close to the BH. We explore the physical regimes where the use of such multiplicative factors is reasonable, and through this introduce a new prescription for gas accretion by BHs. Feedback from AGN is modeled by coupling a fraction of the rest-mass energy of the accreted gas thermally into the surrounding medium. We describe the implementation as well as the limitations of the model in detail and motivate all the changes relative to previous work. We demonstrate how general physical considerations can be used to choose many of the parameters of the model and demonstrate that the fiducial model reproduces observational constraints.

We employ a large suite of cosmological simulations, in which the parameters of the BH model are varied away from their fiducial values, to investigate the robustness of the predictions for the cosmic star formation history and the redshift zero cosmic BH density, BH scaling relations, and galaxy specific star formation rates. We find that the freedom introduced by the need to increase the predicted accretion rates by hand, the standard procedure in the literature, is the most significant source of uncertainty. Our simulations demonstrate that supermassive BHs are able to regulate their growth by releasing a fixed amount of energy for a given halo mass, independent of the assumed efficiency of AGN feedback, which sets the normalization of the BH scaling relations. Regardless of whether BH seeds are initially placed above or below the BH scaling relations, they grow onto the same scaling relations. AGN feedback efficiently suppresses star formation in high-mass galaxies.

Key words: Cosmology: Theory – Galaxies: Active – Galaxies: Evolution – Galaxies: Formation – Hydrodynamics – Galaxies: Quasars: General

1 INTRODUCTION

Over the past decades a growing body of observational and theoretical evidence has suggested that supermassive black holes (SMBHs; $m_{\text{BH}} > 10^6 M_{\odot}$) exist in the centers of all galaxies with spheroids (e.g.

* E-mail: booth@strw.leidenuniv.nl (CMB)

Kormendy & Richstone 1995; Ferrarese & Merritt 2000) and that the properties of these SMBHs are tightly correlated with the properties of the spheroid in which they reside. For example, the mass of the SMBH is found to be tightly correlated with the bulge stellar mass or luminosity (Magorrian et al. 1998; McLure & Dunlop 2002; Haring & Rix 2004; Laor 2001), stellar velocity dispersion (Gebhardt et al. 2000; Merritt & Ferrarese 2001; Tremaine et al. 2002), and galaxy concentration, as measured by the Sérsic index (Graham & Driver 2007). Some recent work has demonstrated that these correlations may be understood in terms of a black hole (BH) ‘fundamental plane’, relating BH mass, galaxy effective radius, stellar velocity dispersion and stellar mass. Here, the mass of the SMBH essentially tracks the binding energy of the stellar bulge (Marconi & Hunt 2003; Feoli & Mele 2005; Aller & Richstone 2007; Hopkins et al. 2007), although other authors argue that the appearance of a fundamental plane is actually due to biasing caused by the presence of galaxies with bars (Graham 2008).

The exact mechanisms leading to the tight observed coupling between galaxy spheroidal components and central active galactic nuclei (AGN) are not yet fully understood, although it has long been recognized that the formation mechanisms of SMBHs (e.g. Silk & Rees 1998) and stars (e.g. Dekel & Silk 1986) are most likely self-regulating. These results suggest that the same processes that shape galaxy spheroids also act on the central BHs. Correlations between AGN activity and other processes provide other clues about the mechanisms that lead to the buildup of the SMBH population. There is evidence that there exists a link between galactic star formation and accretion onto a central AGN: in a global sense, the evolution of the cosmic star formation rate (e.g. Madau et al. 1996) and the luminosity density of quasars are tightly correlated (Boyle & Terlevich 1998). Additionally, on the scale of individual objects it has been found that the most powerful narrow line AGN are preferentially found in galaxies that appear to have undergone a recent starburst phase (Kauffmann et al. 2003).

The massive BHs present in the centres of galaxies are likely to have started their lives as ‘seed’ BHs. The typical masses of seed BHs remains somewhat uncertain, and depends upon the mechanism by which they form. Plausible mechanisms include the collapse of population III stars, giving rise to BHs with masses in the range $10^2 M_\odot < m_{\text{BH}} < 10^3 M_\odot$ (e.g. Madau & Rees 2001; Islam et al. 2003; Schneider et al. 2002), and direct collapse of matter in high redshift, low angular momentum haloes, which may give rise to seed BHs with masses $\sim 10^5 M_\odot$ (e.g. Loeb 1994; Bromm & Loeb 2003; Begelman et al. 2006; Dijkstra et al. 2008; Volonteri & Natarajan 2009). These seed mass BHs can then grow either by mergers with other BHs (e.g. Islam et al. 2003), or through accretion of gas and/or stars.

Accretion of matter onto central BHs, accompanied by the release of a fraction of the rest mass energy of the fuel, has long been recognized as one of the most likely mechanisms to power AGN (Salpeter 1964), and a coupling between the accretion history of an AGN and the gas dynamics of the bulge provides a plausible mechanism by which AGN and bulge properties could become strongly correlated coupled (e.g. Silk & Rees 1998). For example, it has been suggested that the central BHs grow until they release suffi-

cient energy to unbind the gas that feeds them from the host galaxy (Fabian 1999). Bursts of AGN activity then expel gas from galaxies and remain quiescent until stellar mass loss replenishes the galaxy’s gas reservoir (Ciotti & Ostriker 2001)

A theoretical link between galaxy mergers and both galaxy-scale starburst events and active AGN phases has been well established and modelled. Galaxy mergers have long been recognized as a mechanism by which gas can potentially be channeled to the centre of a galaxy (Toomre & Toomre 1972), and N-body simulations of galaxy mergers confirmed and extended this picture by showing that the asymmetrical gravitational potential present during mergers is capable of funneling gas efficiently to the center of a galaxy (Mihos & Hernquist 1994), where it may be accreted by a SMBH. Hydrodynamical simulations of galaxy mergers (Barnes & Hernquist 1991, 1996; Mihos & Hernquist 1996; Kapferer et al. 2005), and numerical models of AGN growth (Kapferer et al. 2005; Springel 2005) predict that these merger events are indeed responsible for the rapid growth of AGN. Recent numerical studies (e.g. Micic et al. 2007) have indicated that both BH mergers and gas accretion are important processes in forming the population of BHs that we observe in the local universe.

Thus, it seems that we can paint a coherent picture in which emission by AGN, galaxy mergers and the growth of supermassive BHs are closely intertwined. As such the study of any one of these processes requires an understanding of all of them. For this reason detailed studies of the co-evolution of the AGN and galaxy populations in a cosmological context often resort to numerical techniques. Early theoretical studies of the galaxy-AGN connection relied upon dark matter halo merger rates, without any separate treatment of galaxy formation processes (Efsthathiou & Rees 1988; Haehnelt & Rees 1993). Later work expanded upon this groundwork by incorporating AGN feedback into semi-analytic modelling of galaxy formation (e.g. Kauffmann & Haehnelt 2000; Cattaneo 2001; Benson et al. 2003; Granato et al. 2004; Croton et al. 2006; Bower et al. 2006; Lagos et al. 2008; Baugh 2006). Semi-analytic models indicate that feedback from AGN is necessary in order to build up a red-sequence of galaxies. Although a combination of photo-heating by reionization and supernova feedback can suppress star formation in low mass haloes – bringing the galaxy luminosity function in line with observations at the low mass end – models without AGN feedback face the problem that the reheated gas in massive haloes would eventually cool, giving rise to an excessive number of bright galaxies (e.g. Bower et al. 2006) as compared to the local universe.

A more computationally challenging approach is to simulate galaxies hydrodynamically, with additional sub-grid modelling of the growth and energy feedback from AGN. Numerical hydrodynamic simulations of galaxy mergers containing AGN (e.g. Springel et al. 2005; Di Matteo et al. 2005; Hopkins et al. 2006; Robertson et al. 2006) have shown that the presence of a central AGN can significantly alter the structure of merger remnants, particularly by expelling a hot halo of diffuse, low-angular momentum gas from the center of the remnant. More recent numerical studies have revealed that dissipation and dry mergers are likely to play a fundamental role in shaping the co-evolution of

BHs and galaxies (Hopkins et al. 2008). Hydrodynamic simulations of full cosmological volumes (Di Matteo et al. 2008; Sijacki et al. 2007; Croft et al. 2008; Okamoto et al. 2008) have probed the effect of AGN on a cosmologically representative set of galaxies and showed that the inclusion of AGN physics into galaxy formation simulations allows us to match many of the observed properties of galaxies in the local universe. The modelling of an AGN population in this manner is both computationally very expensive and subject to very many, as yet poorly understood, numerical effects. As such studies of this type must take care to test the robustness of the models to all physical and numerical parameters.

The focus of the current work is to present and test a new model for the co-evolution of BHs and galaxies. We note that nearly all BH models published thus far in the literature employ the star formation and supernova feedback models of Springel & Hernquist (2003) (hereafter SH03), and the model for BH growth and AGN feedback of Springel et al. (2005)¹ (hereafter S05). Throughout this paper we highlight similarities and differences between our approach and that used previously in the literature. The primary difference between our models and previous work is that we employ a different parametrization of the process of gas accretion onto BHs as well a different implementation of AGN feedback. We show that changes to the BH accretion model can lead to profound differences in galaxy properties, global star formation rates and BH demographics. We examine both the global properties of the simulation, such as the integrated star formation rate and cosmic BH density, and consider the properties of individual galaxies, including specific star formation rates, and the BH fundamental plane. We quantify how uncertainties in our numerical model and all of our parameter choices affect the reliability of our results. We find that changes in the numerical model that generates seed mass BHs, and in the model that distributes feedback energy into the ISM do not strongly affect our results. However, the accretion model is found to be of crucial importance in understanding our results. Throughout we assume a flat Λ CDM cosmology with the cosmological parameters: $\{\Omega_m, \Omega_b, \Omega_\Lambda, \sigma_8, n_s, h\} = \{0.238, 0.0418, 0.762, 0.74, 0.951, 0.73\}$, as determined from the WMAP 3-year data (Spergel et al. 2007) and consistent² with the WMAP 5-year data (Komatsu et al. 2008). Where necessary, observational results have been scaled to our chosen cosmology, and the stellar initial mass function (IMF) assumed in observational analyses has been scaled to the Chabrier IMF used in our simulations.

The paper is structured as follows: In Sec. 2 we introduce our simulation set, and describe briefly the sub-grid physics modules that are not directly related to BHs. In Sec. 3 we describe in detail our model for BH formation, growth and feedback and we motivate our choices for numerical parameters in Sec. 4. In Sec. 5 we present simulation results, including a comparison with redshift zero observational data and an investigation into the severity of uncertainties introduced by different parameter choices. Finally, in Sec. 6 we discuss and summarize our findings. In a com-

panion work we investigate in detail the interplay between feedback from AGN and other feedback processes, including winds driven by Type 2 supernovae and mass loss from the stellar population.

2 NUMERICAL SIMULATIONS

In this section we introduce the numerical techniques used in our simulations and provide a brief overview of the sub-grid physics modules that are not directly related to BH growth or AGN feedback.

We have carried out a suite of cosmological simulations using Smoothed-Particle Hydrodynamics (SPH) (Lucy 1977; Gingold & Monaghan 1977; Monaghan 1992), employing a significantly extended version of the parallel PMTree-SPH code GADGET III (Springel 2005; Springel, Yoshida & White 2001), a Lagrangian code used to calculate gravitational and hydrodynamic forces on a particle-by-particle basis. The initial particle positions and velocities are set at $z = 127$ using the Zel'dovich approximation to linearly evolve positions from an initially glass-like state. The production simulations used in this study are run in boxes of size 50 comoving Mpc/ h , and contain 256^3 particles of both gas and dark matter. Comoving gravitational softenings are set to $1/25$ of the mean comoving inter-particle separation down to $z = 2.91$, below which we switch to a fixed proper scale of 2 kpc/ h . The production simulations have gas particle masses of $8.64 \times 10^7 M_\odot/h$. The boxes are evolved all the way to redshift zero.

In addition to hydrodynamic forces we treat star formation, supernova feedback, radiative cooling, chemodynamics, black hole accretion, and AGN energy feedback in these simulations.

Star formation is tracked in the simulations following the prescription of Schaye & Dalla Vecchia (2008). Gas with densities exceeding a critical density for the onset of the thermo-gravitational instability (hydrogen number densities $n_H = 10^{-2} - 10^{-1} \text{ cm}^{-3}$) is expected to be multiphase and to form stars (Schaye 2004). Because we lack both the physics and the resolution to model the cold interstellar gas phase, we impose an effective equation of state (EOS) with pressure $P \propto \rho^{\gamma_{\text{eff}}}$ for densities $n_H > n_H^*$ where $n_H^* = 0.1 \text{ cm}^{-3}$, normalised to $P/k = 10^3 \text{ cm}^{-3}\text{K}$ at the threshold. We use $\gamma_{\text{eff}} = 4/3$ for which both the Jeans mass and the ratio of the Jeans length to the SPH kernel are independent of the density, thus preventing spurious fragmentation due to a lack of numerical resolution (Schaye & Dalla Vecchia 2008). As described in Schaye & Dalla Vecchia (2008), gas on the effective EOS is allowed to form stars at a pressure-dependent rate that reproduces the observed Kennicutt-Schmidt law (Kennicutt 1998) by construction, renormalised by a factor³ $1/1.65$ to account for the fact that it assumes a Salpeter IMF whereas we use a Chabrier IMF.

Energy injection due to supernovae is included through kinetic feedback. We employ the prescription of Dalla Vecchia & Schaye (2008), which is a variation of the

¹ Although see Okamoto et al. (2008) for a different approach.

² Our value of σ_8 is 1.6σ lower than allowed by the WMAP 5-year data.

³ This normalization factor is calculated from the asymptotic ratio of the numbers of ionizing photons predicted from models of stellar populations with a constant SFR (Bruzual & Charlot 2003).

SH03 recipe for kinetic feedback. In this prescription core-collapse supernovae locally inject kinetic energy and kick gas particles into winds. The feedback is specified by two parameters: Firstly, the initial mass-loading $\eta = \dot{m}_w/\dot{m}_*$, which describes the initial amount of gas put into the wind, \dot{m}_w , as a function of the local SFR, \dot{m}_* , and secondly the wind velocity, v_w . We use $\eta = 2$ and $v_w = 600$ km/s, which corresponds to 40% of the total amount of supernova energy. In contrast with the models of SH03, the kinetic energy is injected *locally* to every star formation event and wind particles are *not* temporarily decoupled from the hydrodynamics when they are put into the wind.

As described in Wiersma et al. (2009b), we follow the timed release of 11 different elements from massive stars (Type II supernovae and stellar winds) and intermediate mass stars (Type Ia supernovae and asymptotic giant branch stars), assuming a Chabrier initial mass function spanning the range 0.1 to 100 M_\odot . Radiative cooling was implemented following Wiersma et al. (2009a)⁴. In brief, net radiative cooling rates are computed element-by-element in the presence of the cosmic microwave background and a Haardt & Madau (2001) model for the UV/X-ray background radiation from quasars and galaxies. The contributions of the eleven elements hydrogen, helium, carbon, nitrogen, oxygen, neon, magnesium, silicon, sulphur, calcium, and iron are interpolated as a function of density, temperature, and redshift from tables that have been precomputed using the publicly available photo-ionization package CLOUDY, last described by Ferland et al. (1998), assuming the gas to be optically thin and in (photo-)ionization equilibrium.

3 THE BLACK HOLE MODEL

We now provide a detailed description of our models for BH formation and accretion (Sec. 3.1), BH mergers (Sec. 3.2) and energy feedback from AGN (Sec. 3.3). Throughout this section we highlight and justify the aspects of our model that differ from previous works. We also introduce all the relevant parameters. In Sec. 4 we motivate our choices for these parameters.

3.1 Black hole formation and accretion

Plausible BH seed formation mechanisms lead to the creation of BHs with masses in the range $10 - 10^5 M_\odot$, whereas SMBHs in the local Universe have masses of up to $10^9 M_\odot$ (see Sec 1 for a discussion). To understand the origin of the redshift zero BH population we therefore need to model how BHs can grow to the sizes observed in present-day galaxies. Over the past decades a picture has emerged in which SMBHs are embedded in dense stellar systems in the centres of galaxies and increase their masses primarily by the accretion of gas (e.g. Begelman & Rees 1978). BHs may also grow by mergers with other BHs, or by the disruption and capture of stars (e.g. Lynden-Bell 1969). The capture of stars has been put forward as an explanation for ultra-luminous

X-ray sources (see e.g. Fabbiano 2006, for a review). However, we neglect this process in the current work, and instead focus on how BHs can accrete gas from their surroundings.

The model presented in this section is a substantially modified version of the model introduced by S05 and employed in almost all of the large-scale numerical simulations of AGN growth thus far available in the literature (see Table 2 for an overview).

Because cosmological simulations have neither the resolution nor the necessary physics to simulate the formation of the seed BHs that eventually grow into SMBHs, it is assumed that low-mass seed BHs are produced sufficiently regularly that every halo above a certain threshold mass contains one such object at its center. Here, our model follows that of Di Matteo et al. (2008) in that we regularly run a friends-of-friends group finder with linking length equal to 0.2 times the initial mean inter-particle spacing (Davis et al. 1985) on all of the dark matter particles during the simulation. We do so at times spaced evenly in log expansion factor, a , such that $\Delta a = 0.02a$, which corresponds to a proper time of ~ 250 Myr (~ 70 Myr) at redshift zero (three) for our cosmology. When a halo grows above some threshold mass, $m_{\text{halo,min}}$, and does not already contain a BH, then its most gravitationally bound baryonic particle is converted into a collisionless BH particle. The initial mass of these BHs is usually chosen to be well below the resolution limit of our cosmological simulations (see Sec. 4), and as such we need to employ sub-grid models to follow the BH. Although we convert the entire particle into a ‘black hole particle’, the mass of the seed BH (m_{seed}) associated with this particle is usually initially significantly less than the particle mass ($m_{\text{seed}} \ll m_g$; where m_g is the simulation gas particle mass). We therefore store the mass of the subgrid BH separately. For the gravitational interactions, other than BH accretion, the full mass of the particle (m_g) is used, but for calculating the BH-specific processes we use the sub-grid BH mass (m_{BH}). We now discuss in more detail the manner in which we track the growth of the BH.

BH particles are collisionless sink particles that contain a sub-grid BH, initially of mass m_{seed} , chosen to be well below the observed mass of BHs in haloes of this size. From their initial seed mass, BHs may grow via one of two processes: mergers with other BHs and accretion of surrounding ambient gas. We now treat each of these processes in turn. In our models BHs accrete from the surrounding ambient gas phase at a rate proportional to that given by the Bondi-Hoyle-Lyttleton (Bondi & Hoyle 1944; Hoyle & Lyttleton 1939) formula

$$\dot{m}_{\text{accr}} = \alpha \frac{4\pi G^2 m_{\text{BH}}^2 \rho}{(c_s^2 + v^2)^{3/2}}, \quad (1)$$

where m_{BH} is the mass of the BH, c_s and ρ are the sound speed and gas density of the local medium, v is the velocity of the BH relative to the ambient medium, and α is a dimensionless efficiency parameter. The factor α did not appear in the original analyses of Bondi & Hoyle (1944) and Hoyle & Lyttleton (1939), but was introduced by S05 as a numerical correction factor, to compensate for the limitations of the numerical simulations. The assumption that BHs grow via Bondi-Hoyle accretion is reasonable even if they are in reality fed by accretion discs that are far smaller than the resolution limit of our simulations as long as the latter grow

⁴ We used their equation (3) rather than (4) and CLOUDY version 05.07 rather than 07.02.

by Bondi-Hoyle accretion. However, we will see that very large factors of α are required for low-mass BHs to grow, in which case one cannot claim to be simulating Bondi-Hoyle accretion.

The amount of accreted mass is related to the rate of growth of the BH by⁵ $\dot{m}_{\text{BH}} = \dot{m}_{\text{accr}}(1 - \epsilon_r)$, where ϵ_r is the radiative efficiency of a BH, which we always assume to be 10%, the mean value for the radiatively efficient Shakura & Syunyaev (1973) accretion onto a Schwarzschild BH.

In order to resolve Bondi-Hoyle accretion onto a BH we need to resolve the Bondi-Hoyle radius (r_b), defined as (e.g. Edgar 2004):

$$r_b = \frac{Gm_{\text{BH}}}{c_s^2} \approx 0.042 \left(\frac{M_{\text{BH}}}{10^6 M_\odot} \right) \left(\frac{c_s}{10 \text{ km/s}} \right)^{-2} \text{ kpc}. \quad (2)$$

Comparing this to the Jeans length,

$$L_J \sim \sqrt{\frac{c_s^2}{G\rho}} \sim \frac{GM_J}{c_s^2}, \quad (3)$$

where M_J is the Jeans mass, we see that $r_b \sim L_J$ if $m_{\text{BH}} \sim M_J$ and $r_b \gg L_J$ if $m_{\text{BH}} \gg M_J$. Hence, any simulation that resolves the Jeans scales will also resolve accretion onto black holes of mass $m_{\text{BH}} > m_g$. We can then parametrize accretion onto a BH in two different ways:

1. Density-Independent Accretion Efficiency:

Most AGN models in the literature use a constant value of $\alpha = 10^2$ (e.g. Springel et al. 2005; Di Matteo et al. 2005; Sijacki et al. 2007; Di Matteo et al. 2008; Bhattacharya et al. 2008; Colberg & di Matteo 2008; Croft et al. 2008; Johansson et al. 2009, see also Table 2). Although most authors do not motivate or even mention⁶ their choice of α , we note that values much greater than unity can be justified in one of two ways: firstly by noting that the Bondi-Hoyle accretion rate depends strongly upon the local ISM sound speed. Galaxy formation simulations currently have neither the resolution nor the physics to self-consistently track the properties of the cold-phase of the ISM, and as such the temperature of the gas accreted by the AGN may be overestimated by orders of magnitude. Hence, we can justify very large values of α in star forming gas. Secondly, in low-resolution simulations we do not resolve the Jeans scale, even in single-phase gas, so the density of the gas at the Bondi radius is underestimated, allowing us to again justify large values of α . We call models that use a fixed value of α ‘constant- α ’ models. Constant- α models are parametrized by a constant multiplicative factor in the

Bondi-Hoyle accretion rate, α_0 . An alternative way of increasing accretion rates is to employ a subgrid model for the unresolved ISM properties, and use this to artificially boost the ISM densities local to the BHs. We discuss this further in the following sections.

We will show in Sec. 4.1 that the use of a constant- α model has a profound effect on the ability of BHs to grow, and that changes in this very poorly constrained parameter can lead to large changes in the global properties of the simulation such as the global density in BHs. We emphasize that values of $\alpha \gg 1$ imply the assumption that the simulation predictions for the gas density and temperature are sufficiently wrong that the Bondi-Hoyle accretion rate is underestimated by two orders of magnitude. Although this assumption can be justified for high-density gas, it does mean that the value of α is in fact more important than the predicted densities and temperatures. One could therefore argue that models of this kind do not really simulate Bondi-Hoyle accretion.

Cosmological simulations can, however, already model Bondi-Hoyle accretion of low-density gas and it hence makes sense to use an accretion model for which the ‘fudge factor’ α becomes unity in the regime where the simulations are reliable. We therefore introduce a new class of black hole accretion models in which the value of α depends on the local gas density, while keeping the number of free parameters fixed.

2. Density-Dependent Accretion Efficiency: The assumptions used to justify large values of α in simulations similar to ours break down when two conditions are satisfied: firstly the local gas density must be lower than required for the formation of a cold (i.e. $T \ll 10^4$ K) phase, and secondly the simulation must resolve the Jeans scale of the single-phase gas. Our highest resolution simulations (as well as many published AGN simulations) do resolve the Jeans scale at the star formation threshold and so in contrast to most published AGN models we choose to parametrize the accretion efficiency parameter as a function of density

$$\alpha = \begin{cases} 1 & \text{if } n_{\text{H}} < n_{\text{H}}^* \\ \left(\frac{n_{\text{H}}}{n_{\text{H}}^*} \right)^\beta & \text{otherwise.} \end{cases} \quad (4)$$

Here, the accretion efficiency (α) becomes unity for densities lower than the critical value required for the formation of a cold interstellar gas phase ($n_{\text{H}}^* = 0.1 \text{ cm}^{-3}$; see Sec. 2). As discussed above, provided the simulations resolve the Jeans scale, the Bondi radius will be resolved for BHs with $m_{\text{BH}} \geq m_g$, which means that values of $\alpha \gg 1$ are unphysical for such BHs. We then choose to parametrize our lack of knowledge about both the physical properties of the multiphase ISM and the rate at which it accretes onto the central AGN using a power-law of the gas density, with slope β . This constant- β model, which has the same number of free parameters (one) as the constant- α models used in previous work, allows us to correctly describe accretion in the physical regime where it is resolved by our simulations and to introduce a reasonable scaling when it is not. We will show in Sec. 5.2 that the change from a constant- α to a constant- β model can have a profound effect on the growth of BHs, particularly for low mass galaxies. We call models of this type ‘constant- β models’.

⁵ Note that S05 neglected the $(1 - \epsilon_r)$ term and used $\dot{m}_{\text{BH}} = \dot{m}_{\text{accr}}$.

⁶ Springel et al. (2005); Di Matteo et al. (2005); Sijacki et al. (2007); Di Matteo et al. (2008); Bhattacharya et al. (2008); Colberg & di Matteo (2008) all do not discuss or mention the value of α that they used, but we have been informed by V. Springel that they assumed $\alpha = 100$. Khalatyan et al. (2008) state explicitly that in their models $\alpha = 300$ and justify this by noting that when the density of the ISM is smoothed on the scale of the computational resolution, the recovered densities are much lower than would be expected on the scale of the Bondi radius. Using similar reasoning, Johansson et al. (2009) reach a similar conclusion and set $\alpha = 100$.

A second approach to boosting accretion rates, which operates in a similar manner to the constant- β models, is to make use of a subgrid model for the unresolved subgrid physics not encapsulated by the simulations. For example, Pelupessy et al. (2007) use the star formation and supernova feedback models of SH03 to estimate the amount of time that a BH spends in dense, molecular clouds, and Okamoto et al. (2008) use a subgrid model in which drag due to stellar radiation on a clumpy ISM can give rise to large accretion rates onto a central BH. We note that differing implementations of the subgrid model can lead to large differences in the properties of the ISM and for the purposes of this work we emphasize that the functional form (Eq. 4), as well as the value for β , are ad-hoc. Any function for which $\alpha \rightarrow 1$ at gas densities for which the simulations are reliable and for which $\alpha \gg 1$ at higher densities would do. We chose to use a simple power-law dependence because it satisfies these constraints, is continuous and uses only one free parameter. We will investigate the effect of changing β in the following sections. In the limit that $\beta \rightarrow 0$ the behaviour of the constant- β model will tend towards that of a constant- α model with $\alpha_0 = 1$, and in the limit that $\beta \rightarrow \infty$ the model tends towards behaviour where the accretion is pure Bondi-Hoyle in non star-forming gas, and always Eddington limited in gas with densities above the star formation threshold. We caution that this prescription is not suitable for simulations that resolve the relevant physics at densities exceeding n_{H}^* .

Because we have changed the density-dependence of the accretion rate, we cannot claim to be simulating Bondi-Hoyle accretion. Values of $\alpha \gg 1$ are, however, motivated by the Bondi-Hoyle formula. Moreover, for $n_{\text{H}} > n_{\text{H}}^*$ the density should be interpreted as the mass-weighted mean density of the unresolved, multiphase medium, smoothed on the scale of the spatial resolution of the simulation, whereas the density appearing in the Bondi-Hoyle formula applies to a single gas phase. Since the accretion rate-weighted mean density (which we can only compute if we know the mass distribution of the multiphase gas as a function of density and temperature) is unlikely to be proportional to this effective density, there is no reason to keep the Bondi-Hoyle scaling. For this reason, and because $\alpha \gg 1$ implies the assumption that the predicted densities and temperatures are greatly in error, we argue that constant- α prescriptions with $\alpha \gg 1$ can no more claim to be modeling Bondi-Hoyle accretion than constant- β prescriptions. We prefer the latter since it allows us to get the right answer in the regime where the simulations are reliable, that is, at sufficiently low densities. Finally, we note that both accretion models use the Bondi-Hoyle scaling of the accretion rate with the mass of the BH, $\dot{m}_{\text{accr}} \propto m_{\text{BH}}^2$.

In common with the models of S05 we limit the accretion rate to the Eddington rate:

$$\dot{m}_{\text{Edd}} = \frac{4\pi G m_{\text{BH}} m_{\text{p}}}{\epsilon_{\text{T}} \sigma_{\text{T}} c}, \quad (5)$$

where m_{p} is the proton mass and σ_{T} is the Thomson cross section for scattering of free electrons. Because $\dot{m}_{\text{Edd}} \propto m_{\text{BH}}$ whereas $\dot{m}_{\text{accr}} \propto m_{\text{BH}}^2$, Eddington limited accretion tends to be more important for more massive BHs.

Following S05, we allow BH particles to stochastically

swallow neighbouring baryonic particles with a probability

$$p_i = \begin{cases} (m_{\text{BH}} - m_{\text{part}}) \rho^{-1} W(r_{\text{BH}} - r_i, h_{\text{BH}}) & \text{if } m_{\text{BH}} > m_{\text{part}} \\ 0 & \text{otherwise} \end{cases}$$

where ρ is the local gas density, m_{BH} is the mass of the subgrid black hole, m_{part} is the mass of the particle containing the sub-grid BH and $W(r_{\text{BH}} - r_i, h_{\text{BH}})$ is the SPH kernel, evaluated between the positions of the BH and gas particle i . The BH smoothing length, h_{BH} , is chosen such that within a distance h_{BH} from the BH there are $N_{\text{ngb}} = 48$ neighbours, the same number of neighbours as we used in our SPH calculations. This process ensures that the mass of the BH particle always closely tracks m_{BH} .

When the mass of the BH particle is smaller than or of the same order of magnitude as the simulation mass resolution, the black hole does not dominate the local dynamics and may wander from the centre of mass of its parent halo due to numerical effects. Conservation of momentum from accreted ISM gas can lead to similar effects. In order to avoid this we employ the same scheme as in the models of S05. At every timestep the gravitational potential energy is calculated at the position of each of the BH's neighbouring gas particles and the BH particle is repositioned on top of the particle with the minimum potential energy. In order to prevent the BH from being 'dragged' by a minimum-potential particle with a large relative velocity, we only perform this process if the relative velocity between the BH and its most-bound gas particle neighbour is less than $0.25 c_s$, where c_s is the local sound speed. This process ensures that the location of the BH particle always tracks the centre of mass of its parent halo very closely. This procedure is halted after the mass of the SMBH becomes greater than ten times the initial gas particle mass in the simulation because by this point the BH dominates the dynamics in the centre of the halo.

3.2 Black hole mergers

Galaxy mergers are thought to be one of the major processes driving the evolution of galaxies. When galaxies merge it is expected that their central BHs will eventually also merge. Indeed, the build-up of BHs through mergers may play an important part in the growth of SMBHs. Similarly to S05 we have implemented BH merging as follows. When any two BHs pass within a distance h_{BH} of each other with a relative velocity smaller than the circular velocity at a distance h_{BH} ($v_{\text{rel}} < \sqrt{Gm_{\text{BH}}/h_{\text{BH}}}$, where h_{BH} and m_{BH} are the smoothing length and mass of the most massive BH in the pair respectively) then they are allowed to merge. This velocity criterion is necessary in order to prevent BHs from merging during a fly-through encounter of two galaxies, as this could lead to BHs being quickly removed from their host galaxies due to momentum conservation. This velocity scale is somewhat different from that employed by S05, who used the local sound speed, c_s , as the relevant velocity scale, arguing that the sound speed represents a simple measure of the characteristic velocity scale of the galaxies, and hence gives a simple measure of the velocity scale at which BHs will be able to merge. However, because AGN input large amounts of energy into their surroundings, it is not necessarily true that the sound speed local to the AGN reflects the depth of the potential well.

The BH merging rate estimated from our simulations likely represents an upper limit to the true merger rate as our simulations do not have the resolution required to resolve the formation of the tight BH binaries that are a prerequisite for their eventual coalescence (Callegari et al. 2008). Since it is not yet fully understood how long it takes to harden a BH binary (Makino & Funato 2004), we assume that the merging process is instantaneous.

3.3 Energy feedback from black holes

The precise mechanism by which energy emitted from a BH is coupled to the surrounding medium is as yet unknown, but plausible mechanisms include radiation pressure on free electrons (which gives rise to the classical Edington limit), Compton heating of the infalling gas (e.g. Ciotti & Ostriker 2001; Wang et al. 2006), photoionization pressure (Buff & McCray 1974; Cowie et al. 1978) and radiation pressure on dust grains (e.g. Murray et al. 2005). Regardless of the precise coupling mechanism, there is a catalogue of observational evidence indicating that energy output from AGN can drive galactic outflows. For example, absorbers seen in X-rays show evidence of outflow (Laor et al. 1997) and broad absorption line systems show evidence of outflows at very high velocity (e.g. Pounds et al. 2003). Although these observations indicate that high velocity outflows are present around some AGN, they do not tell us how much mass (and hence how much energy) is present in the outflow. Estimates of the mass outflow rate in the winds are highly uncertain. Some studies (e.g. Chelouche 2008) imply that the actual rate of mass outflow is only a small fraction of the bolometric luminosity of the AGN sources, while other studies (e.g. Arav et al. 2002, 2008) suggest large mass outflow rates in quasar driven winds.

In our models BHs inject a fixed fraction of the rest mass energy of the gas they accrete into the surrounding medium. The feedback is implemented thermally, that is: energy is deposited into the surrounding gas by increasing its internal energy, as opposed to the kinetic feedback used to inject supernova energy, which is deposited by kicking the gas particles (see Sec. 2). The fraction of the accreted rest mass energy that is injected is assumed to be independent of both the environment and the accretion rate. We thus do not differentiate between ‘quasar mode’ and ‘radio mode’ feedback as in the models of Sijacki et al. (2007). In a future work we will consider how spatially distributed AGN heating mechanisms affect the cosmological evolution of galaxies. The amount of energy returned by a BH to its surrounding medium in a timestep Δt is given by

$$E_{\text{feed}} = \epsilon_f \epsilon_r \dot{m}_{\text{BH}} c^2 \Delta t, \quad (6)$$

where ϵ_f is the efficiency with which a BH couples the radiated energy into its surroundings – a free parameter in our simulations – and c is the speed of light. Only the product of ϵ_r and ϵ_f is important in calculating the amount of energy feedback in our model.

Because our sub-grid model for SF relies on an effective EOS and does not include a (semi-)analytic sub-grid model for the multiphase ISM, our energy distribution mechanism is different from that in S05. In contrast, because we prefer to minimize the use of semi-analytic models within our

hydrodynamical simulations, our models rely only on an effective EOS and leave the distribution of the mass over unresolved gas phases undefined. We therefore need to make two changes to the EOS model of Schaye & Dalla Vecchia (2008) that was used in our simulations without AGN feedback.

Firstly, in the original models, once gas was identified as star-forming it was forced to remain on the EOS, until its density dropped below the critical density for star-formation, n_{H}^* , it turned into a star particle, or it was kicked into the wind. It is therefore necessary that we change this by allowing strongly heated gas to leave the EOS. This is implemented numerically by taking gas that is heated by more than 0.5 dex above the EOS in a single time step off the EOS (i.e. it is no longer star-forming and its pressure is no longer constrained to lie on the EOS). Gas is placed back onto the EOS if its temperature falls back below 0.5 dex above the EOS temperature corresponding to its density. By checking SFRs, both globally and for individual objects, and by comparing gas distributions on the $\rho - T$ plane we have verified that making this change to our EOS model has a negligible effect on the results in a simulation that does not include AGN feedback. A second possible change to the AGN model would have been to treat the effective EOS as a lower limit to the gas temperature. We tested this and again found the differences in our results to be negligible. We choose to use the first procedure in order to facilitate direct comparisons between the simulations containing AGN and those run earlier in the project.

Secondly, in order to ensure that the thermal feedback from BHs is not immediately radiated away it is necessary to impose a *minimum heating temperature*. BHs store feedback energy until they have accumulated enough energy to increase the temperature of n_{heat} of their neighbours by an amount of ΔT_{min} , i.e.

$$E_{\text{crit}} = \frac{n_{\text{heat}} m_{\text{g}} k_{\text{B}} \Delta T_{\text{min}}}{(\gamma - 1) \mu m_{\text{H}}}, \quad (7)$$

where E_{crit} is the critical energy for a heating event to be triggered and μ is the mean molecular weight of the gas (we assume $\mu = 0.58$, appropriate for a fully ionized gas of primordial composition). The internal energy of the heated gas is instantaneously increased by an amount E_{crit} . This implementation of quasar mode feedback is similar to the radio mode feedback introduced by Sijacki et al. (2007). If ΔT_{min} is set too low then the cooling time of the AGN heated gas will remain very short, and the energy will be efficiently radiated away. If $n_{\text{heat}} \Delta T_{\text{min}}$ is set too high then the threshold energy for a heating event to occur and hence the time period between AGN heating events will become very large. In particular, a time interval larger than the Salpeter time would prevent the BH from regulating its growth. Finally, we note that the energy is deposited into the ambient gas isotropically, equally distributed to a random fraction $n_{\text{heat}}/N_{\text{ngb}}$ of the BH’s neighbours. If, on a given timestep, a BH accretes more energy than necessary to heat n_{heat} particles to ΔT_{min} then the process is repeated until the BH has distributed all of its energy, so individual gas particles may be heated by an amount ΔT_{min} multiple times on a given timestep.

4 PARAMETER CHOICES

Both the mechanism by which BHs grow and the efficiency of their thermal feedback can be changed drastically by changing the values of the parameters of the AGN model. In this section we discuss how parameter values are chosen to minimize unphysical numerical effects whilst simultaneously requiring that the global properties of the BH distribution satisfy various observational constraints. For quick reference, Table 1 contains a full list of the parameters that control the behaviour of the BH growth and AGN feedback model, along with their fiducial values.

Because it is difficult to discuss the effect of each parameter in isolation, we will first discuss the general properties of the BH model (e.g. growth mechanisms, feedback efficiency) and use each of these general themes to motivate our fiducial choices for the parameters of the AGN model.

4.1 Black hole growth

We allow BHs to grow by two processes: mergers with other BHs and accretion of gas. The BH accretion time-scale $t_{\text{accr}} \equiv m_{\text{BH}}/\dot{m}_{\text{BH}}$ is, for Bondi-Hoyle accretion (Eq. 1), proportional to m_{BH}^{-1} . Therefore, depending upon choices for various parameters, the initial growth of BHs can proceed in one of two different ways. Firstly, in the regime where the time scales over which gas accretion operates are very long, BHs may grow primarily by mergers with other (seed mass) BHs until m_{BH} is large enough for the accretion rate to become appreciable. In this regime black holes initially grow at a rate governed by the integrated mass of seed BHs they collide with. Secondly, seed mass BHs may have accretion rates large enough for the BHs to experience runaway growth until their accretion rate is limited by feedback processes.

We can estimate the growth rate of BHs by noting that in our star formation model we impose an effective equation of state on star-forming gas, and as such can immediately calculate the local ISM pressure, P , (and hence $c_s = \sqrt{\gamma P/\rho}$) from

$$P = P_{\text{crit}} \left(\frac{n_{\text{H}}}{n_{\text{H}}^*} \right)^{\gamma_{\text{eff}}}, \quad (8)$$

where $n_{\text{H}}^* = 0.1 \text{ cm}^{-3}$ and P_{crit} are the critical threshold density and pressure for star formation respectively (see Sec. 2). Fig. 1 shows BH growth times as a function of the ambient gas density for both constant- α and constant- β models, assuming here that the BH is of mass $10^6 M_{\odot}$. For the purposes of this plot we assume that when gas densities are below the star-formation threshold the EOS is isothermal, but note that in the simulations we calculate the pressure self-consistently. Following other authors, we set $\alpha_0 = 100$ for the constant- α model. For the constant- β lines we set $\beta = [1, 2, 4]$. The horizontal, red line in this plot shows the growth time of a BH that is accreting at the Eddington rate (i.e. the Salpeter time). The Salpeter time depends only upon physical constants and the BH radiative efficiency, such that

$$t_{\text{Salpeter}} \equiv \frac{m_{\text{BH}}}{\dot{m}_{\text{Edd}}} = \frac{\epsilon_r \sigma_{\text{T}} c}{4\pi G m_{\text{p}}} = 4.5 \times 10^5 \left(\frac{\epsilon_r}{0.1} \right) \text{ yr}. \quad (9)$$

It is immediately clear from Fig. 1 that the choice of accretion model strongly affects the local density at which the BH

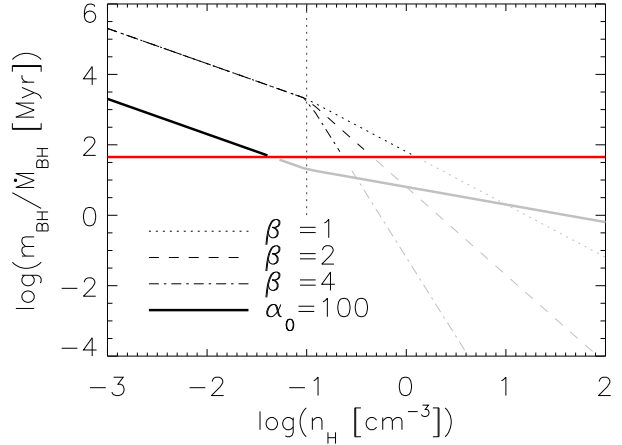


Figure 1. BH growth times ($m_{\text{BH}}/\dot{m}_{\text{BH}}$) as a function of the ambient gas density under various accretion models, all for a BH mass of $10^6 M_{\odot}$. The normalization of all black lines scales as m_{BH}^{-1} . Lines are shown for both a constant- α accretion model (solid, black/grey line) and for constant- β accretion models (all other black/grey lines). The solid, red line shows the Salpeter time (the growth time for a BH accreting at the Eddington rate), and represents the lower limit on the BH growth time in the simulations. The grey section of each line represents the region where the accretion rate is greater than the Eddington rate. The vertical dotted line shows the star formation density threshold, $n_{\text{H}}^* = 10^{-1} \text{ cm}^{-3}$. Above this density the gas follows the effective equation of state defined by Eq. 8. For lower densities we have assumed the gas to be isothermal (only in this figure, not in the simulations). Note that the constant- α accretion model predicts that a $10^6 M_{\odot}$ BH will be growing at an Eddington limited rate even in gas with density at the star-formation threshold (0.1 cm^{-3}).

growth becomes Eddington limited, with black holes accreting in the constant- α model becoming Eddington limited at densities 1-2 orders of magnitude lower than the same black hole accreting in the constant- β model.

From the simulations we find that, for our chosen value of $m_{\text{halo,min}} (=100 m_{\text{DM}}$; see Sec. 4.3) and at high redshift, typical birth densities of BHs are $\sim 10 - 100$ times the star formation threshold. Hence, in the regimes of interest, in constant- α models all BHs of mass $> 10^5 M_{\odot}$ grow initially at close to the Eddington rate⁷ (for a seed mass of $10^5 M_{\odot}$ and typical initial gas densities of $10^1 - 10^2 \text{ cm}^{-3}$ the initial Eddington ratio is 0.037-0.37) until feedback effects reduce the local gas density to values below the threshold for star formation. From Fig. 1 we can see that for a BH of mass $10^6 M_{\odot}$ the accretion rate remains Eddington limited until the local gas density falls to $n_{\text{H}} \lesssim 10^{-2} \text{ cm}^{-3}$. Fig. 2 presents this information in a slightly different manner by showing the density above which a BH's accretion rate is Eddington limited as a function of BH mass for the same accretion mod-

⁷ Note that the choice of sub-grid ISM model is a significant source of additional uncertainty in the accretion rates. For example, the use of the SH03 sub-grid multi-phase ISM can give rise to differences of almost an order of magnitude in the accretion rates of seed mass black holes due to the use of different effective equations of state.

Table 1. Full list of parameters of the AGN model, along with the values they take in the fiducial set of simulations, and short definitions.

Parameter	Fiducial Value	Description
m_{seed}	$0.001 m_g$	Initial mass of the sub-grid BH
$m_{\text{halo,min}}$	$100 m_{\text{DM}}$	Minimum halo mass into which BH seeds may be placed
ϵ_r	0.1	Radiative efficiency of the BH accretion discs
ϵ_f	0.15	Fraction of energy emitted by BHs that couples into the ambient gas
n_{heat}	1	Number of neighbouring particles heated per feedback event
ΔT_{min}	10^8 K	Amount by which BH feedback heats surrounding gas
		Depending on the accretion model, one of the following parameters is used:
α_0	100	Normalization of the Bondi-Hoyle accretion efficiency (Eq. 1) <i>in constant-α models</i>
β	2	Slope of the Bondi-Hoyle accretion efficiency (Eq. 4) <i>in constant-β models</i>

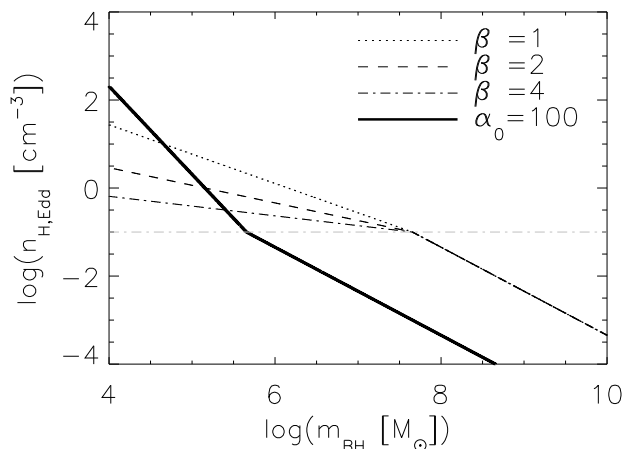


Figure 2. The gas density above which the accretion rate onto a black hole becomes Eddington limited as a function of BH mass, assuming that gas with density above the critical density for star formation, $n_{\text{H}}^* = 10^{-1} \text{ cm}^{-3}$ has properties governed by the effective EOS and that gas below the critical density follows an isothermal EOS. The thick, black line shows the behaviour of a constant- α accretion model, and all other lines show how models with a constant- β accretion rate behave. The grey line shows the critical density for star formation in our simulations. Except for very low BH masses, the constant- α model becomes Eddington limited at much lower gas densities than the constant- β models.

els as in Fig. 1. Again, it is clear that the gas density below which the accretion rate depends on the density, and can thus more easily be regulated by feedback from the AGN, has a strong dependence on the accretion model used. Take, for example, the case of a BH of mass $10^8 M_{\odot}$, here in a constant- α model this BH will grow at the Eddington rate until it can modulate its local density to below $10^{-3.5} \text{ cm}^{-3}$, more than two orders of magnitude below the star-formation threshold. This is well within the regime where Bondi-Hoyle accretion is resolved in the simulations.

In the constant- α model with $\alpha_0 = 100$ the growth of BHs therefore proceeds as follows: Seed mass BHs (typical seed masses are in the range $10^3 - 10^5 M_{\odot}$ in our simulations) grow exponentially by Eddington limited accretion until feedback from the BH has decreased the local ISM density to the point that growth is no longer Eddington limited, and further energy output from the AGN can decrease the accretion rate. For BHs with masses greater than $10^6 M_{\odot}$ self-regulation can only occur at densities orders of

magnitude below the star formation threshold (Fig. 2). In this regime we resolve Bondi-Hoyle accretion, invalidating the assumption used to justify large values of α in the first place.

In contrast, simulations that employ a constant- β model, are not necessarily Eddington limited from birth. Taking again the case of a $10^6 M_{\odot}$ BH, and our fiducial value of $\beta = 2$, we see that the BH can decrease its accretion rate at a much higher gas density, and as such the period of Eddington limited growth will be much shorter than for the constant- α model. The difference in the gas density below which AGN accretion rates are no longer Eddington limited can lead to large differences in the properties of low mass galaxies and BH growth in small haloes.

4.2 Efficient thermal feedback

As discussed in Sec. 3.3, it is necessary to impose a minimum heating temperature in order to prevent BHs from heating their surroundings before they have generated enough energy for thermal feedback to become efficient.

Two parameters control how efficient this feedback may be: the number of neighbours to heat (n_{heat}) and the temperature to which the neighbours are heated (ΔT_{min}). Two competing effects control our choices for these parameters. If ΔT_{min} is too low then AGN heated gas will retain a low temperature and therefore also a short cooling time (an analogous problem to the ‘overcooling’ of supernova heated gas in early cosmological simulations (Katz et al. 1996), which is, however, usually attributed to an overestimate of the gas density). In this regime the energy will be immediately radiated away, making AGN feedback ineffective. Conversely, if ΔT_{min} or n_{heat} are set too high then the time scale over which BHs accrete enough energy to heat n_{heat} of their neighbours by an amount ΔT_{min} will become longer than either the dynamical time in the vicinity of the BH (or the Salpeter time for Eddington limited growth), leading to spurious growth as BHs are unable to self-regulate.

The choice of the minimum heating temperature, ΔT_{min} , is motivated by the fact that we wish to choose the minimum value (and so minimum time between heating events) for which the cooling time of the heated gas is long enough that the energy is not immediately radiated away. In practice it was found that $\Delta T_{\text{min}} = 10^8$ K is the minimum temperature for which BH feedback has a sufficient effect on galaxy clusters. We return to this point in Sec. 5.2.

The second parameter, n_{heat} , is calibrated by noting that although ideally we would like to allow AGN to heat

gas instantaneously, our finite resolution forces us to store energy until the feedback is effective, hence introducing a delay to AGN heating. We can minimise the effect of this delay by noting that the numerically imposed time between heating events should be lower than the typical time-scales of dynamical processes that affect AGN feedback. If n_{heat} is set too high then it is possible that the amount of time taken for a BH to accrete enough energy to perform a heating event would be large enough that we see spurious growth. We can quantify this effect by calculating the mean time between heating events for BHs of different masses in different density environments. This is demonstrated in Fig. 3, which shows the mean time between heating events as a function of $m_{\text{BH}}/m_{\text{g}}$ for models with both constant- β and constant- α accretion rates. Plotting the heating time as a function of this mass ratio allows us to make this plot in a resolution independent manner. Fig. 3 assumes $\Delta T_{\text{min}} = 10^8$ K and $n_{\text{heat}} = 1$, but all lines can be shifted vertically in proportion with the quantity $\Delta T_{\text{min}} n_{\text{heat}}$. To make the time between feedback events as small as possible we should choose n_{heat} as small as possible, but it is not immediately obvious that BHs will be able to regulate their growth if we heat only a small number of neighbours of an AGN that it will be able to self-regulate. However, we found from numerical tests (Sec. 5.2) that $n_{\text{heat}} = 1$ is sufficient for BH feedback to be effective, and so $n_{\text{heat}} = 1$ is the parameter value used in our fiducial simulations. The dependence of our results on the two parameters ΔT_{min} and n_{heat} will be discussed in Sec. 5.2.

The next model parameter is ϵ_{f} , the efficiency with which energy radiated from the BH is coupled to the ISM. The parameter ϵ_{f} sets the normalizations of the global BH density and the BH-galaxy scaling relations. We therefore tune ϵ_{f} after setting all of the other parameters in order to match the redshift zero observations (Sec. 5.2, Fig. 7d) and find that a value of $\epsilon_{\text{f}} = 0.15$ provides a good match to the observations.

4.3 Black hole seed mass and minimum halo mass

Our initial choice for the halo mass into which we insert a BH is motivated by the fact that we wish for every resolved halo with $m_{\text{halo}} \gg m_{\text{seed}}$ to contain a seed BH. We therefore choose to place BH seeds into haloes of a constant particle number. Using $m_{\text{halo, min}} = 100 m_{\text{DM}}$ ensures that haloes containing BHs are always well defined (e.g. Diemand et al. 2007). The choice of a constant particle number halo mass also has the advantage that if we change the simulation mass resolution, BHs will still be placed into the smallest allowable mass of dark matter haloes without the need to tune any parameters. Note, however, that this prescription will have to be changed for simulations that have sufficient resolution for $100 m_{\text{DM}}$ to be comparable or smaller than the minimum halo mass expected to be able to form seed mass BHs.

Given the minimum halo mass into which we place BH seeds, we must ensure that the integrated number of seed BHs generated between redshifts $z = \infty$ and zero is much smaller than the observed cosmic BH density. We can obtain an upper limit on the cumulative cosmic density of BH seeds by taking the redshift zero dark matter halo mass function $f(m) = n(m)dm$ assuming that *all* collapsed mass was as-

sembled through mergers of critical mass haloes:

$$\rho_{\text{seed}}(m_{\text{halo, min}}) < \frac{m_{\text{seed}}}{m_{\text{halo, min}}} \int_{m_{\text{halo, min}}}^{\infty} m f(m) dm. \quad (10)$$

This quantity is plotted for a number of values of the seed BH mass in Fig. 4, where the two vertical grey lines represent the masses of haloes of 100 DM particles ($=m_{\text{halo, min}}$) in our fiducial simulations run at the mass resolution as the OWLS runs of Schaye et al. (in preparation).

Given choices for ΔT_{min} and n_{heat} , we can use Fig. 3 to place a minimum limit on the BH seed mass, m_{seed} . Here, we show the time between heating events as a function of BH mass, for both constant- α and constant- β models. The time between heating events for BHs accreting at the Eddington accretion rate are shown as red lines in each panel. We now note that we require BH heating to occur regularly in high density environments. In particular, in order for a BH to be able to effectively self-regulate its own growth, we require that the numerically imposed minimum duty-cycle, Δt_{heat} , is less than the Salpeter time, the characteristic growth time for black holes accreting at the Eddington rate. It is clear from Fig. 3 by comparing the BH Salpeter time (blue line) to the BH duty cycle that in high density environments ($n_{\text{H}} > 10^2 \text{ cm}^{-3}$) this condition is satisfied only if the BH mass is greater than $10^{-3} m_{\text{g}}$. This provides a minimum allowed seed mass in our models.

However, in addition to ensuring that BHs grow in a physical manner and that their feedback can be effective, we must also satisfy various observational constraints. Most fundamentally, it is known that the present day cosmic BH density is $(4.2 \pm 1.1) \times 10^5 M_{\odot}/\text{Mpc}^3$ (Shankar et al. 2004) or $(4.22^{+1.75}_{-1.22}) \times 10^5 M_{\odot}/\text{Mpc}^3$ (Marconi et al. 2004), although we caution that a more accurate consideration of the effects of cosmology may lead to a slightly higher determination of the BH density (Graham & Driver 2007b). In order that we do not violate these observational constraints in the presence of substantial BH growth through accretion, we require the $z = 0$ global seed density to be much smaller than the observed BH mass density. We now ensure that – given all of our other parameter choices – $m_{\text{seed}} = 10^{-3} m_{\text{g}}$ does not violate this constraint on the global BH density. For our simulations $10^{-3} m_{\text{g}}$ corresponds to a BH seed mass of $1.2 \times 10^5 M_{\odot}$. It is clear from Fig. 4 that the maximum possible contribution of the seed BH mass to the cosmic density is at least a factor of 10 less than the redshift zero observations, which we indicate by the grey, horizontal shaded region. We will see in Fig. 7 that, as expected, the actual contributions of seed BHs to the total cosmic density are much smaller than this value.

An additional observational constraint is placed by the well-defined relation between the mass of a BH and the mass of the bulge component of a galaxy, $m_{\text{BH}} \approx 0.006 m_{\text{bulge}}$ (Magorrian et al. 1998). In simulations it is more convenient to work with the relation between BH mass and dark matter halo mass, investigated by Ferrarese (2002), who found that in halos of $10^{12} M_{\odot}$ the ratio $m_{\text{BH}}/m_{\text{halo}} \sim 10^{-5}$. This provides a second, related constraint on the mass of seed BHs: we wish to place them below this relationship so that they can subsequently grow on to the observed redshift zero relation⁸. For our parameter choices ($m_{\text{seed}} = 10^{-3} m_{\text{g}}$ and

⁸ In some BH seed generation scenarios, for example the direct

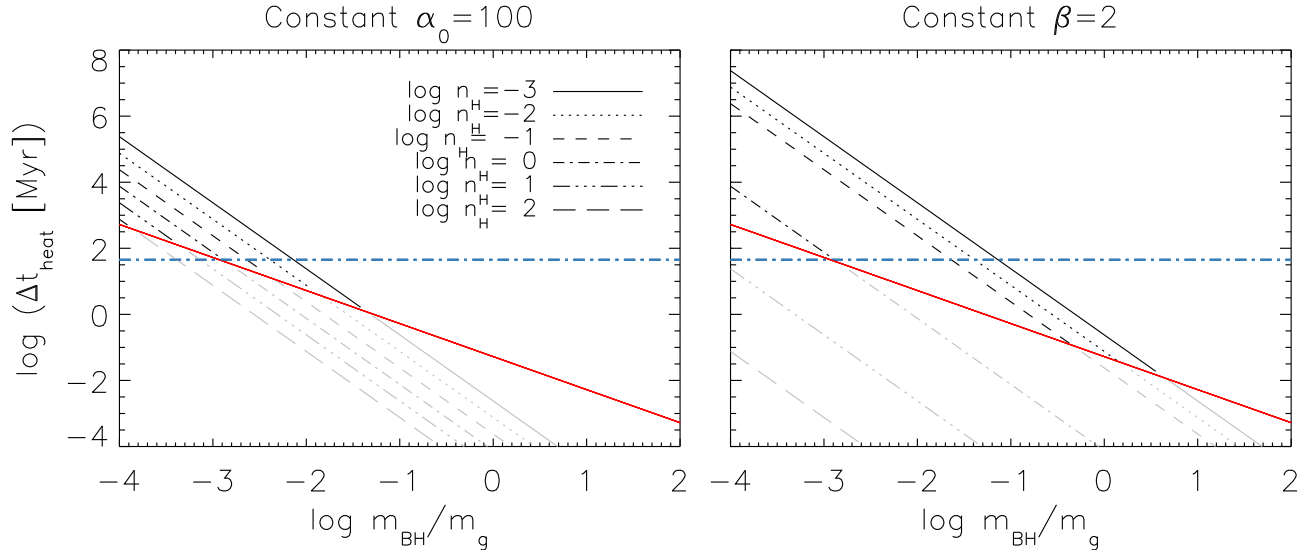


Figure 3. Time between AGN heating events for Bondi-Hoyle (black and grey lines) and Eddington-limited (red lines) accretion as a function of the ratio between the BH mass and the simulation gas particle mass. The grey section of each line represents the region where $\dot{m} > \dot{m}_{\text{Edd}}$. In this plot we assume that $n_{\text{heat}} = 1$ and $\Delta T_{\text{min}} = 10^8$ K. All lines may be shifted vertically in proportion with $n_{\text{heat}} \Delta T_{\text{min}}$. The horizontal blue line shows the Salpeter time ($m_{\text{BH}}/\dot{m}_{\text{Edd}}$). *Left panel:* A constant- α accretion model with $\alpha_0 = 100$. *Right panel:* A constant- β accretion model with $\beta = 2$. The spacings between the lines change when $n_{\text{H}} > n_{\text{H}^*}$, because the accretion efficiency becomes proportional to n_{H}^β . For any Eddington limited accretion and BH masses greater than $10^{-3} m_{\text{g}}$ the time between heating events is shorter than the Salpeter time, enabling the BHs to self-regulate.

$$m_{\text{halo},\text{min}} = 100 m_{\text{DM}}$$

$$\frac{m_{\text{seed}}}{m_{\text{halo},\text{min}}} = \frac{10^{-3}}{100} \left(\frac{\Omega_b}{\Omega_m - \Omega_b} \right) = 2.1 \times 10^{-6}, \quad (11)$$

where the last equality assumes our chosen cosmology. This ratio is indeed much smaller than the observed value.

Finally, we note that our fiducial choice of seed mass, $m_{\text{seed}} = 10^{-3} m_{\text{g}}$, will need to be modified for simulations that have sufficient resolution for this value to be below the expected BH seed masses.

4.4 Comparison with previous work

Through the arguments in the previous sections we were able to specify values for all of our model parameters. These fiducial parameter values are summarised in Table 1. The AGN model developed in this paper is a modification of that introduced in S05, and used thereafter in a large number of works. As such it is instructive to compare our parameter choices with those employed in other studies, as collected in Table 2.

We turn our attention first to the AGN feedback efficiency, ϵ_f . The value used in the present study ($\epsilon_f = 0.15$) is significantly higher than that used in previous published studies, which all assume $\epsilon_f = 0.05 - 0.1$. We can account for this difference if we note that, unlike the other studies, we do not employ the SH03 subgrid model for the ISM. Use

collapse of matter in haloes we expect BH seeds to reside initially above the observed scaling relations. We will show in Sec. 5.2.2 that in our models BHs grow onto the BH scaling relations regardless of whether they are initially placed above or below the relations.

of a different subgrid model for the unresolved ISM is likely to lead to differences in the amount of radiative losses, as the effective density and temperature of the ISM differ significantly between the two models.

We note that apart from differences in the ISM model and AGN heating mechanisms, the strength of the AGN feedback depends only on the parameter combination $\epsilon_r \epsilon_f$, and that there is significant leeway in the value of ϵ_r . All studies presented in Table 2 assume $\epsilon_r = 10\%$, but values close to $\epsilon_r = 20\%$ are possible for thin-disc accretion on to a Kerr BH (Yu & Tremaine 2002; Thorne 1974). Recent observational determinations of ϵ_r span the full range of allowable values: $\epsilon_r = 30 - 35\%$ (Wang et al. 2006), $\epsilon_r = 15\%$ (Elvis et al. 2002; Yu & Lu 2008), $\epsilon_r = 7 - 8\%$ (Cao & Li 2008; Martinez-Sansigre & Taylor 2008) depending upon the specific assumptions and models used in each study.

The ratio of the minimum halo mass to the seed mass is similar in all of the cosmological studies, with the exception of the work of Khalatyan et al. (2008), who performed zoomed cosmological simulations of an individual object. In order to avoid numerical issues when $m_{\text{BH}} < m_{\text{g}}$, these authors forced the BH to accrete very quickly at early times before artificially halting its accretion until the stellar mass of the halo becomes large enough that the BH lies on the observed $m_{\text{BH}} - m_*$ relation.

We see also from Table 2 that the minimum halo mass ($m_{\text{halo},\text{min}}$) is consistent between all of the published cosmological studies to within a factor of 5 ($1 - 5 \times 10^{10} M_{\odot}$). We will show in Sec. 5.2 that, for the constant- α accretion model assumed in previous studies, AGN feedback affects all haloes into which seed mass black holes are placed, and that changing $m_{\text{halo},\text{min}}$ by a factor of ten has a large ef-

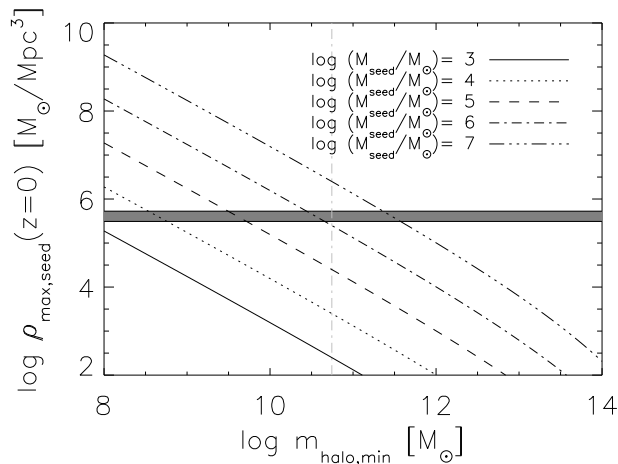


Figure 4. Maximum possible contribution to the cosmic BH density from seed mass BHs, as a function of the minimum dark matter halo mass, $m_{\text{halo,min}}$, assuming the dark matter mass function of Reed et al. (2006). Each black line corresponds to a different BH seed mass, as indicated in the legend. The horizontal, grey shaded region shows the observed cosmic black hole density at redshift $z = 0$ (Shankar et al. 2004), and the vertical line indicates $m_{\text{halo,min}}$ for our fiducial simulation, which has a DM mass resolution of $8.64 \times 10^{-7} M_{\odot}$. For our fiducial BH seed mass of $m_{\text{seed}} = 1.2 \times 10^{-5} M_{\odot}$ we see that the maximum possible contribution of seed mass BHs to the global BH density is much lower than the $z = 0$ observations.

fect on the BH properties of the less massive haloes in the simulation. Care should therefore be taken when comparing results of different simulations.

The two areas where our work differs most from previous models are the BH accretion model and the SN feedback model. We turn our attention first to the SN model and note that almost all previous studies employ the work of SH03, whereas we use the method of Dalla Vecchia & Schaye (2008). Contrary to SH03, SN winds in our model are local and not hydrodynamically decoupled from the surrounding gas. Hydrodynamical decoupling of supernova heated gas, as implemented in the SH03 model, guarantees that when gas is kicked it is able to escape the ISM (although it may subsequently return). On the other hand, if the hydrodynamic forces are taken into account, the gas can remain confined by pressure forces, and if it does manage to escape it may drag along much of its neighbouring gas. It was shown in Dalla Vecchia & Schaye (2008) that in high-resolution simulations of individual disc galaxies this change fundamentally alters the structure of the galactic disc and that hydrodynamically coupled winds and generate galactic outflows with properties broadly comparable with observations. We demonstrate in a companion work that SN feedback has a large effect on the properties of the AGN population and, as such, it is important to investigate a number of SN feedback prescriptions.

The second area where our model differs significantly from others in the literature is in the accretion model. In the nomenclature of this paper, all of the previous AGN models are constant- α accretion models in which $\alpha_0 = 100\text{--}300$. We show in later sections that the accretion model represents one of the most crucial elements of an AGN model, and

that all results are very sensitive to the way in which BHs are allowed to accrete.

We show in this work that the results derived from simulations depend on aspects of the BH model that are homogeneous between the studies that have thus far been published. The present work – which is carried out using different techniques and parametrizations for much of the sub-grid modelling – therefore provides a way to investigate the robustness of the models.

5 SIMULATION RESULTS

In this section we first introduce the simulation set used in this paper (Sec. 5.1) before demonstrating that the fiducial simulations reproduce redshift zero observational results and quantifying how robust our model is to poorly constrained parameter choices (Sec. 5.2). To begin with, however, we show for illustrative purposes the gas density in a 3 Mpc/h thick slice from our 100 Mpc/h (*L100N512*) simulation at redshift zero (Fig. 5). Each panel represents a successive factor of five zoom. The bottom-left panel shows a region 800 kpc/h across, centered on a $3 \times 10^7 M_{\odot}$ BH, contained in a halo with a stellar mass of $3 \times 10^{10} M_{\odot}$ and a dark matter mass of $2 \times 10^{12} M_{\odot}$. Circles in this plot represent the locations of BHs with the area of each circle proportional to the logarithm of the mass of the BH.

5.1 Simulation list

In order to explore parameter space we have run a large number of smaller simulations, the details of which are summarised in Table 3. Simulation names are of the form *LxxxNyyy*, where *xxx* represents the simulation box size in comoving Mpc/h and *yyy* is the cube root of the initial number of dark matter and gas particles. For example, the simulation denoted *L100N512* refers to a comoving simulation volume of 100 Mpc/h, which contains 512^3 dark matter particles and an equal number of baryonic particles. Simulations for which one of the parameters was changed from its default value are denoted by appending a descriptive suffix to the end of the simulation name. For example, simulations without AGN feedback are named *LxxxNyyyNOAGN*, and correspond to the simulations denoted *REF.LxxxNyyy* in the OWLS project (Schaye et al., in preparation).

5.2 The effects of changing the model parameters

We now turn our attention to the effect of varying each of the parameters of our AGN model away from those selected in Sec. 4. In order to quantify the effect of different aspects of the AGN model on the results of our simulation, we split the model parameters into four separate categories: the accretion model (α_0 ; β); the seed generation model ($m_{\text{halo,min}}$; m_{seed}); the feedback efficiency (ϵ_f); and the heat distribution model (ΔT_{min} ; n_{heat}). We look separately at the effects of changes in each of these parameter sets, and additionally consider two purely numerical effects: the simulation mass resolution and box size. For each set of simulations we make four diagnostic plots: in Fig. 6 we show the cosmic SFR density as a function of redshift; Fig. 7 shows the evolution of the global BH density, and the cumulative BH density

Table 2. Model parameters for AGN feedback studies in the literature. Columns are as follows: 1) Reference; 2) Efficiency with which energy emitted by a BH is coupled into the ambient gas; 3) Radiative efficiency of BH accretion discs; 4) Multiplication factor for the Bondi-Hoyle accretion rate; 5) For star forming gas the Bondi-Hoyle accretion rate is multiplied by $(n_{\text{H}}/10^{-1} \text{ cm}^{-3})^\beta$ (Eq. 4); 6) Mass of seed BHs; 7) Minimum halo mass in which black hole seeds are placed; 8) Number of DM particles corresponding to a halo of mass $m_{\text{halo,min}}$, ranges indicate the difference between the highest and lowest resolution simulations used in each study; 9) The ratio of the BH seed mass to the minimum halo mass; 10) Type of simulation: Iso., isolated model disc galaxy. Zoom, zoomed simulation of individual object in a cosmological volume. Cosmo., uniform mass resolution simulation of a cosmological volume; 11) Reference for star formation model used in the study: Springel & Hernquist (2003) (SH03), Schaye & Dalla Vecchia (2008) (SD08); 12) Reference for supernova wind model used in this study: Springel & Hernquist (2003) (SH03), Dalla Vecchia & Schaye (2008) (DS08)

Study (1)	ϵ_f (2)	ϵ_r (3)	α_0 (4)	β (5)	$\frac{m_{\text{seed}}}{M_\odot}$ (6)	$\frac{m_{\text{halo,min}}}{M_\odot}$ (7)	$N_{\text{halo,min}}$ (8)	$\frac{m_{\text{seed}}}{m_{\text{halo,min}}}$ (9)	Type (10)	SF Model (11)	Wind Model (12)
Springel et al. (2005)	0.05	0.1	100	0	10^5	n/a	n/a	n/a	Iso.	SH03	SH03
Robertson et al. (2006)	0.05	0.1	100	0	10^5	n/a	n/a	n/a	Iso.	SH03	SH03
Sijacki et al. (2007)	0.05	0.1	100	0	10^5	5×10^{10}	2260	2×10^{-6}	Zoom	SH03	SH03
Sijacki et al. (2007)	0.05	0.1	100	0	10^5	5×10^{10}	285-606	2×10^{-6}	Cosmo.	SH03	SH03
Johansson et al. (2008)	0.05	0.1	100	0	10^5	n/a	n/a	n/a	Iso.	SH03	SH03
Di Matteo et al. (2008)	0.05	0.1	100	0	10^5	1×10^{10}	36-363	1×10^{-5}	Cosmo.	SH03	SH03
Khalatyan et al. (2008)	0.1	0.1	300	0	n/a	n/a	1463	n/a	Zoom	SH03	SH03
This study	0.15	0.1	1	2	$10^{-3} m_g$	$100 m_{\text{DM}}$	100	2×10^{-6}	Cosmo.	SD08	DS08

Table 3. Summary of simulation parameters. Columns are as follows: 1) Name of simulation; 2) Comoving box size; 3) Number of DM and gas particles; 4) Final redshift; 5) Multiplication factor for the Bondi-Hoyle accretion rate (Eq. 1); 6) For star forming gas the Bondi-Hoyle accretion rate is multiplied by $(n_{\text{H}}/10^{-1} \text{ cm}^{-3})^\beta$ (Eq. 4); 7) Fraction of radiated energy that is coupled back into the ISM (Eq. 6); 8) Initial mass of sub-grid BH; 9) Minimum halo mass into which a seed BH is placed; 10) Minimum AGN heating temperature difference; 11) Number of particles heated per event. Entries in boldface represent parameters that have been changed from the value they take in the default model.

Identifier (1)	$\frac{L}{\text{Mpc}/h}$ (2)	N_{gas} (3)	z_{end} (4)	α_0 (5)	β (6)	ϵ_f (7)	$\frac{m_{\text{seed}}}{m_g}$ (8)	$\frac{m_{\text{halo,min}}}{m_{\text{DM}}}$ (9)	$\frac{\Delta T_{\text{heat}}}{10^8 \text{ K}}$ (10)	n_{heat} (11)
Simulations for parameter studies										
<i>L050N256</i>	50.0	256^3	0	1	2	0.15	0.001	100	1	1
<i>L050N256VLOEPS</i>	50.0	256^3	0	1	2	0.0375	0.001	100	1	1
<i>L050N256LOEPS</i>	50.0	256^3	0	1	2	0.075	0.001	100	1	1
<i>L050N256HIEPS</i>	50.0	256^3	0	1	2	0.3	0.001	100	1	1
<i>L050N256VHIEPS</i>	50.0	256^3	0	1	2	0.6	0.001	100	1	1
<i>L050N256HIHALO</i>	50.0	256^3	0	1	2	0.15	0.001	1000	1	1
<i>L050N256HISEED</i>	50.0	256^3	0	1	2	0.15	0.01	100	1	1
<i>L050N256LOSEED</i>	50.0	256^3	0	1	2	0.15	0.0001	100	1	1
<i>L050N256HINHEAT</i>	50.0	256^3	0	1	2	0.15	0.001	100	1	10
<i>L050N256B0</i>	50.0	256^3	0	1	0	0.15	0.001	100	1	1
<i>L050N256B1</i>	50.0	256^3	0	1	1	0.15	0.001	100	1	1
<i>L050N256B4</i>	50.0	256^3	0	1	4	0.15	0.001	100	1	1
<i>L050N256A100B0</i>	50.0	256^3	0	100	0	0.15	0.001	100	1	1
<i>L050N256A1000B0</i>	50.0	256^3	0	1000	0	0.15	0.001	100	1	1
<i>L050N256T7</i>	50.0	256^3	0	1	2	0.15	0.001	100	0.1	1
<i>L050N256NOAGN</i>	50.0	256^3	0	–	–	–	–	–	–	–
Simulations for box size and resolution tests										
<i>L100N128</i>	100.0	128^3	0	1	2	0.15	0.001	100	1	1
<i>L100N128NOAGN</i>	100.0	128^3	0	–	–	–	–	–	–	–
<i>L100N256</i>	100.0	256^3	0	1	2	0.15	0.001	100	1	1
<i>L100N256NOAGN</i>	100.0	256^3	0	–	–	–	–	–	–	–
<i>L100N512</i>	100.0	512^3	0	1	2	0.15	0.001	100	1	1
<i>L100N512NOAGN</i>	100.0	512^3	0	–	–	–	–	–	–	–
<i>L025N128</i>	25.0	128^3	0	1	2	0.15	0.001	100	1	1

present in seed-mass BHs (grey curves); Fig. 8 shows the redshift zero $m_{\text{BH}} - M_*$ and $m_{\text{BH}} - \sigma$ relations. We associate BHs with gravitationally bound objects by identifying bound substructures in the simulation using the algorithm SUBFIND (Springel et al. 2001; Dolag et al. 2008). We note

that in this plot we show *total* halo stellar mass as a function of BH mass, as opposed to the observations, where only the bulge stellar mass is calculated. This means that all curves can be shifted slightly to the left. Finally, Fig. 9 shows the median specific SFR (SSFR) in bins of stellar mass. In this

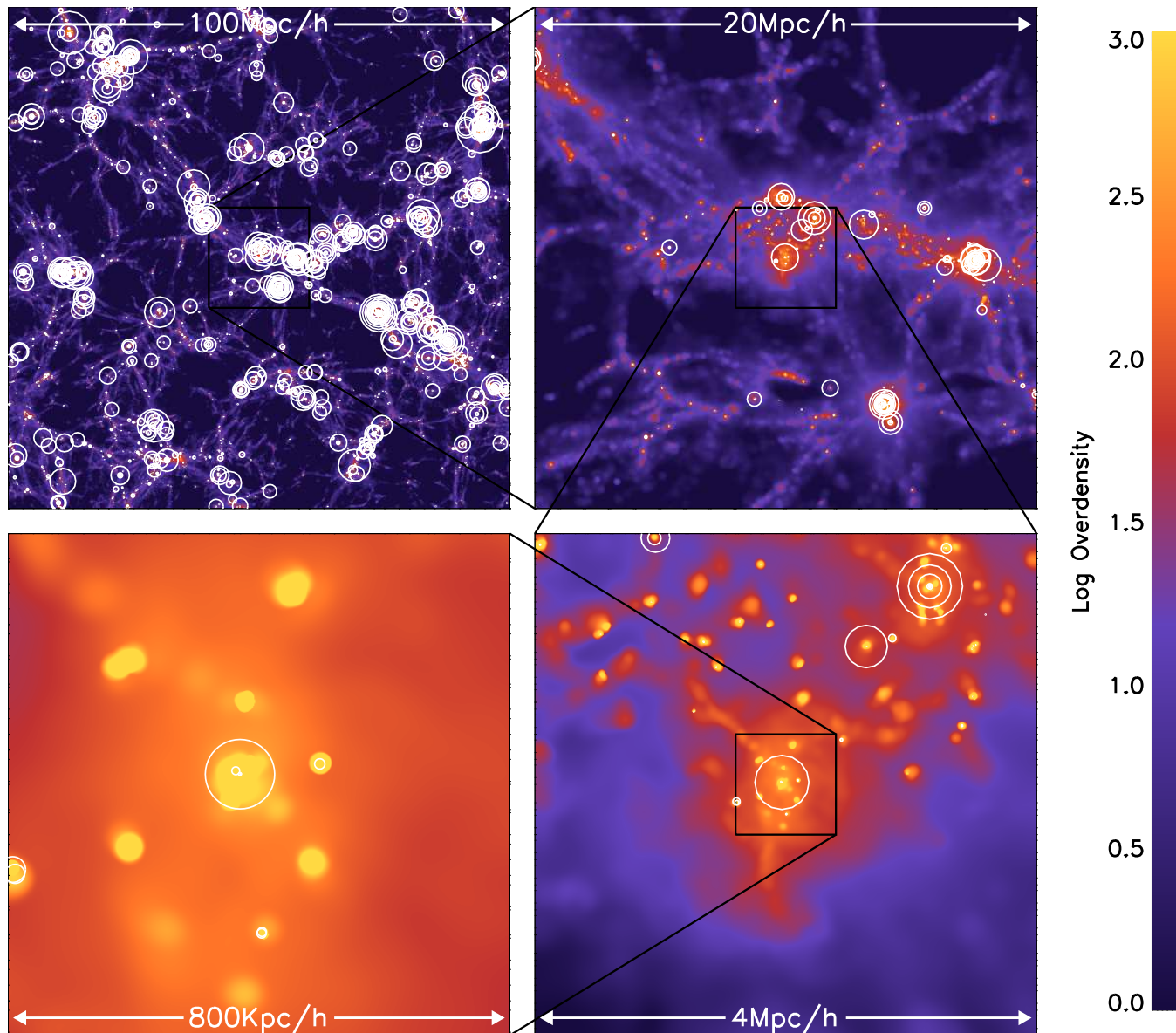


Figure 5. Successively zoomed projections of the gas density in a $3 \text{ Mpc}/h$ thick slice from our *L100N512* simulation at redshift zero. BHs are represented in this plot by open circles and the area of each circle is proportional to the logarithm of the BH mass. The largest circle in the lower-left panel represents a BH of mass $3 \times 10^7 M_{\odot}$.

plot, the grey lines represent results from simulations that do not include AGN feedback. In figures 9 and 8 the vertical lines represent the halo stellar masses at with 50% and 90% of haloes contain BHs massive enough to have performed at least one heating event. It is immediately clear from Fig. 8 that the $m_{\text{BH}} - \sigma$ relation is much more robust to changes in parameters than the $m_{\text{BH}} - M_{*}$ relation.

Each set of simulations is compared to our fiducial simulation (*L050N256*), which uses the model parameters that were justified in Sec. 4. To aid comparison between the different simulation sets, the fiducial simulation appears in every plot as a solid, black curve. Details of all the simulations discussed in this section appear in Table 3. We now discuss each simulation set in turn.

5.2.1 The effect of box size and mass resolution

We consider first the effect of changing the box size at a constant resolution by comparing models *L100N512*, *L050N256* and *L025N128*. The size of the simulation box has a negligible effect on both the star formation rate density (Fig. 6a) and, for $z < 4$, on the global mass of BHs (Fig. 7a). Because the properties of individual BHs are set by local physical processes, increasing the box size does nothing to the scaling relations (Fig. 8a), except for allowing us to probe the mass function up to larger halo masses. The same holds true for the SSFRs of individual objects (Fig. 9a).

We now assess the impact of numerical resolution on our results. We compare simulations at three different resolutions (*L100N512*, *L100N256*, and *L100N128*) both with and without AGN feedback. Simulation *L100N128* has a

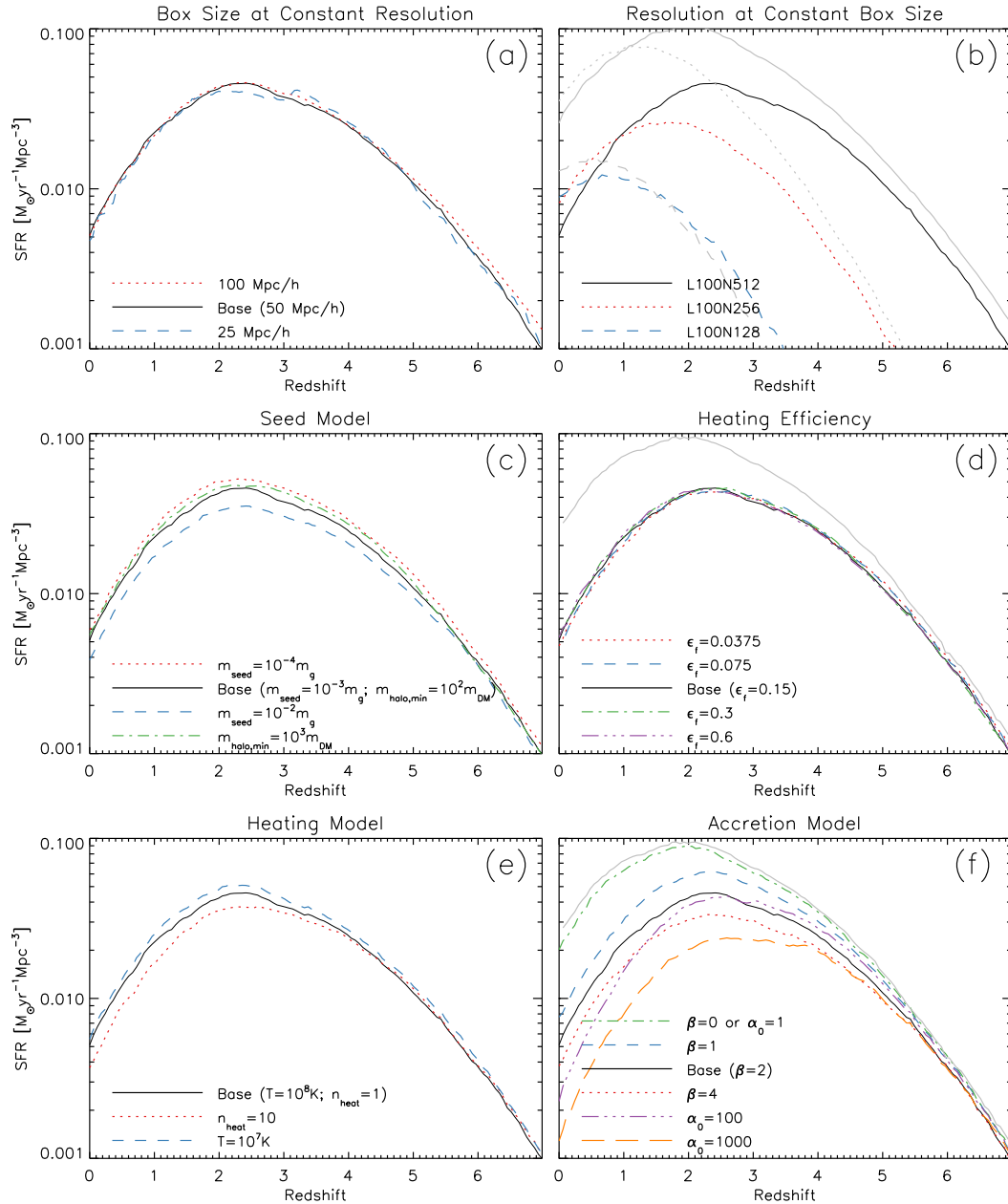


Figure 6. The dependence of the global star formation history on various sets of parameters. (a): The effect of changing the simulation volume at a constant resolution; (b): The effect of changing the resolution at a constant box size; (c): Simulations with different prescriptions for the generation of seed BHs ($m_{\text{halo,min}}$, m_{seed}); (d): Simulations with different values of the heating efficiency (ϵ_f); (e): The effect of changing the way in which AGN feedback energy is distributed to the surrounding gas particles (ΔT_{min} , n_{heat}); (f): The effect of changing the BH accretion model (α_0 , β). Curves in grey represent simulations that do not include AGN feedback and the solid black curve in each panel represents the fiducial simulation (*L050N256*).

dark matter particle mass of $3.54 \times 10^{10} M_{\odot}$, a factor of 64 worse than that used in *L050N256*, our lowest resolution production simulation.

We concentrate first on the star formation history in these simulations (Fig. 6b). At high redshift ($z > 4$), the star formation rate is governed by numerical resolution. At low redshift ($z < 2$) the two highest resolution simulations (*L100N512* and *L100N256*) have star formation rates that differ by ~ 0.2 dex, indicating that this quantity is not yet

fully resolved. We see by comparing simulations with and without AGN that the factor by which AGN feedback decreases the global SFR is the same in both simulations. However, in the lowest resolution simulation (*L100N128*; blue, dashed line), the AGN are largely ineffective at decreasing the global SFR.

We now turn our attention to the BH properties. The $z < 1$ integrated BH density (Fig. 7b) is virtually indistinguishable between runs *L100N512* and *L100N256*. This

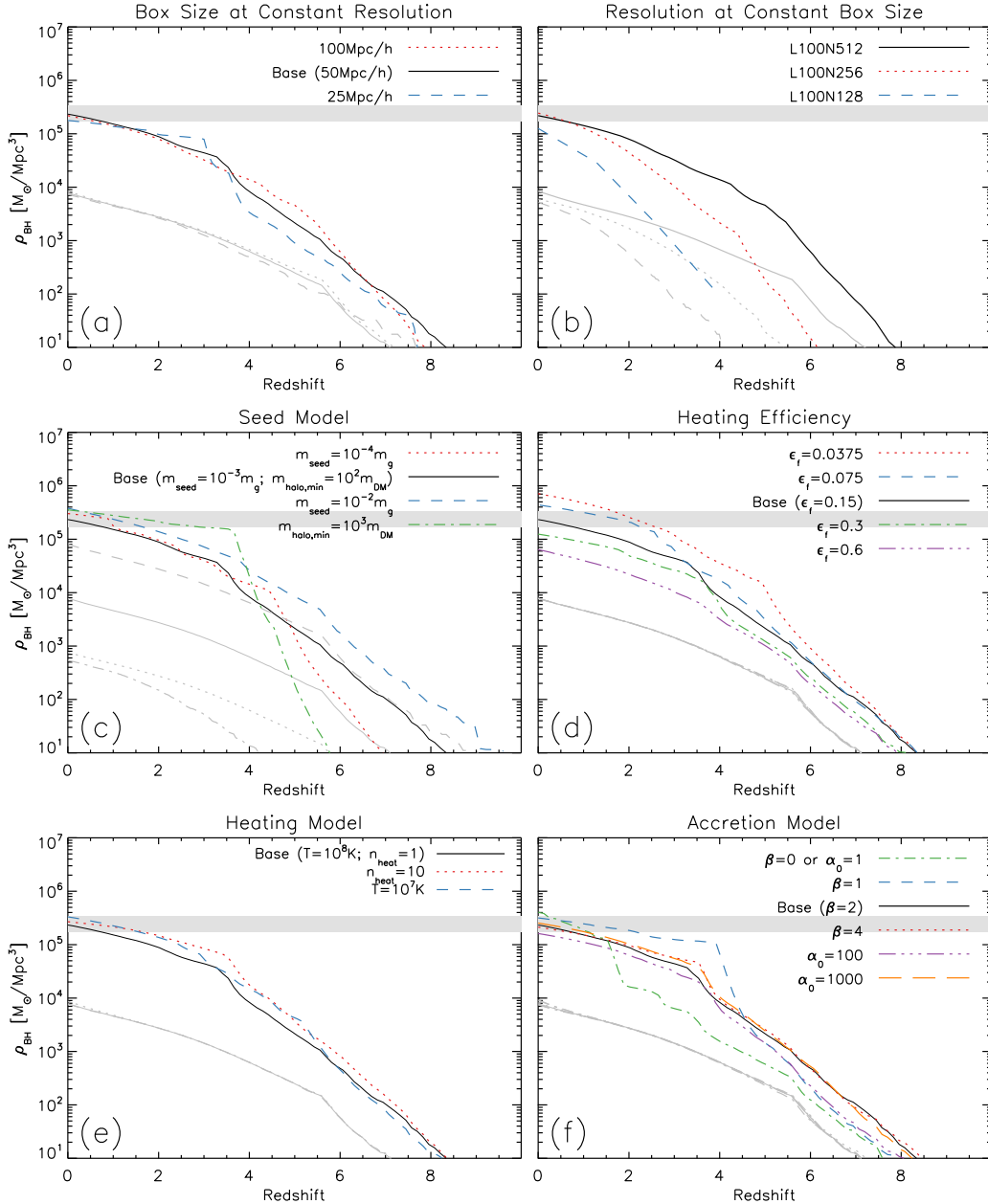


Figure 7. The dependence of the evolution of the the cosmic BH density on the parameters of the AGN model. The panels are the same as in Fig. 6, the shaded grey area represents the redshift zero BH density as measured by Shankar et al. (2004). The grey curves show the cumulative density in seed BHs. The solid, black curve in each panel represents the fiducial simulation (*L050N256*).

occurs because the global black hole density is dominated by the massive BHs, which are well resolved in both simulations. *L100N128* underpredicts the redshift zero BH density by a factor of two. This is due to two reasons. Firstly, in this simulation seed mass BHs are placed only in objects with masses larger than $3.54 \times 10^{12} M_{\odot}$, which means that we neglect a large population of important black holes. Secondly, we see that the first BHs in this simulation start growing only at low redshift ($z \approx 4$), and as such, may not have had enough time to grow onto the observed BH scaling relations.

This picture is borne out by the properties of individual BHs. Fig. 8b shows that for $\sigma > 100$ km/s the BH proper-

ties are well converged, whereas at the lower mass end of the scaling relations the resolution becomes important. The lowest resolution simulation underpredicts the BH scaling relations at all masses.

If we now examine the SSFRs of individual objects (Fig. 9b), looking first at simulations that do not contain AGN (*L100N512NOAGN* and *L100N256NOAGN*; grey, dotted and solid lines respectively) we see that the SSFR is almost converged above a stellar mass of $10^{10.5} M_{\odot}$. If we now consider the effect of adding AGN feedback to these simulations, we see that the stellar mass at which the simulations with and without AGN diverge from one another has

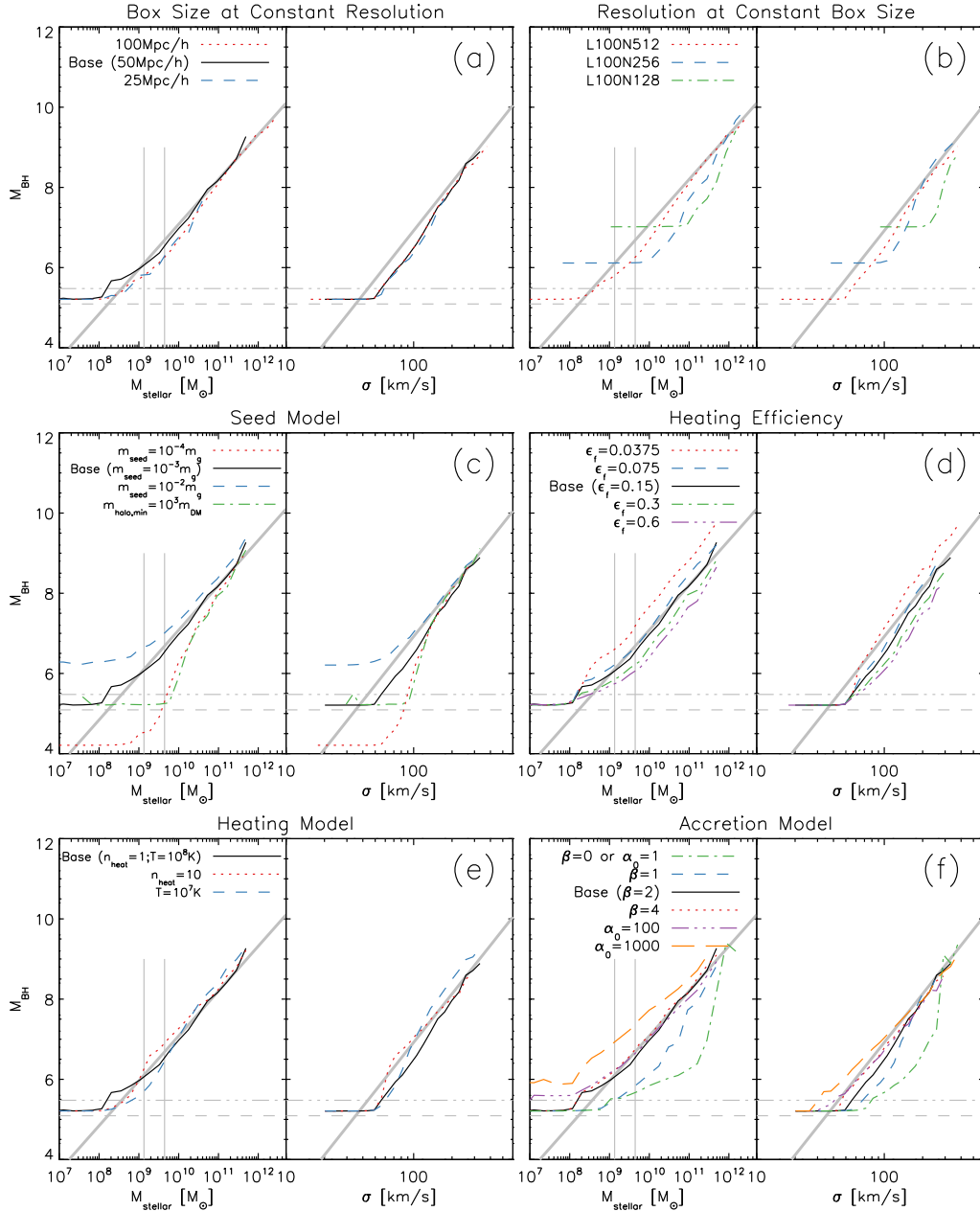


Figure 8. The Magorrian relation and the $m_{\text{BH}} - \sigma$ relation for each set of simulations. Line styles and panels correspond to those in Fig. 6. The simulated stellar velocity dispersion is calculated as the mean of the three one-dimensional velocity dispersions of the stellar particles in each halo. The pale, solid, grey line in each plot represents the redshift zero observations of Haring & Rix (2004) (left panel) and Tremaine et al. (2002) (right panel). The solid, black curve in each panel represents the fiducial simulation (*L050N256*). The horizontal, triple-dot-dashed line indicates the mass that a BH requires to begin to heat its surroundings, and the horizontal grey, dashed line indicates the black hole seed mass in the fiducial simulation. The two solid vertical lines show, for the fiducial simulation, the stellar mass above which 50% and 90% of haloes contain a BH massive enough to have performed at least one heating event.

not yet converged, indicating that results on the scale of individual objects in these simulations may remain affected by numerical resolution. We note that the redshift zero global SFR is affected by resolution to a lesser degree than the SSFR. This is likely to be because the total galaxy stellar mass is an integral over all time of the galaxy star formation rates, so the strong resolution effects at high redshift (Fig. 6b) persist in the redshift zero population.

We thus conclude that, because local processes govern the size of individual BHs, the simulation box size is unimportant when discussing BH scaling relations. However, the limited simulation mass resolution means that the stellar masses in our simulated galaxies are not yet fully resolved. We also conclude that BH properties, such as the integrated cosmic mass density and BH scaling relations are converged in all of our production simulations, but decreasing the mass

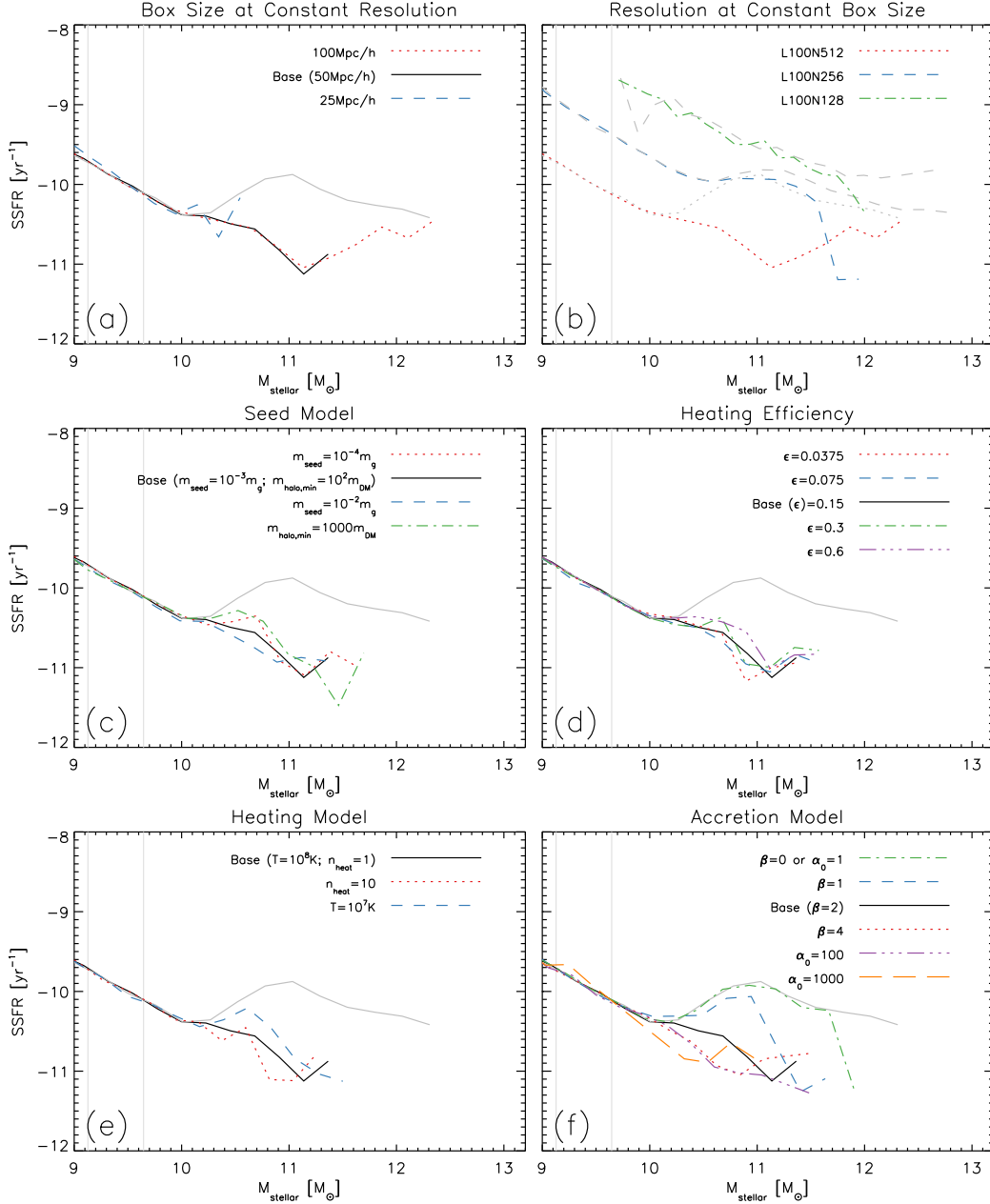


Figure 9. The median SSFR as a function of galaxy stellar mass for each set of simulations. Line styles and panels correspond to those in Fig. 6. The pale, grey curve in each plot represents the SSFR as measured in the simulation without AGN feedback (*L050N256NOAGN*). The solid black curve in each panel represents the fiducial simulation (*L050N256*). The upturn in galaxy SSFR in the simulations without AGN feedback at $M_* \approx 3 \times 10^{10} M_\odot$ is due to SN feedback becoming inefficient. The two vertical lines in each panel indicate, for the fiducial simulation, the stellar mass above which 50% and 90% of haloes contain a BH massive enough to have performed at least one heating event.

resolution by a factor of 64 places us in the regime where no AGN properties are resolved. Therefore, we can conclude that the global results we present in this paper are robust to changes in numerical resolution, but that predictions involving the stellar properties of individual objects should be treated with caution.

5.2.2 The seed model

Two parameters control the way that seed BHs are generated: the BH seed mass (m_{seed}) and the halo mass above which BH seeds are inserted into haloes ($m_{\text{halo,min}}$). For the minimum halo mass we chose to use a fixed number of particles, $m_{\text{halo,min}} = 100m_{\text{DM}}$, rather than a fixed halo mass because this ensures that BHs are always placed into well defined haloes, regardless of the numerical resolution. Con-

sideration of the AGN feedback process then allowed us to place a minimum value on the possible mass of BH seeds ($10^{-3} m_g$) such that the average time between heating events for a BH accreting at the Eddington rate is shorter than the Salpeter time, making it possible for the BH to regulate its growth. We also noted that the requirement that the total mass in seed mass BHs generated in a simulation is much lower than the observed redshift zero cosmic BH density, does not allow the seed mass to be much larger than the minimum possible value. We thus chose $m_{\text{seed}} = 10^{-3} m_g$ as our fiducial value. We now examine how changes in these two parameters affect our results.

By comparing our base model (*L050N256*) to a simulation in which BH seeds are only placed into haloes that are ten times more massive (*L050N256HIHALO*; green dot-dashed curves) we can say that most of our results are insensitive to the choice of $m_{\text{halo,min}}$. The global star formation rate density in the simulations (Fig. 6c) is virtually unaffected by changing $m_{\text{halo,min}}$ from $10^2 m_{\text{DM}}$ to $10^3 m_{\text{DM}}$, probably because the SFR of galaxies is only affected by AGN in the most massive haloes ($M_* \gtrsim 10^{11} M_\odot$; Fig. 9). The cosmic BH density is also insensitive to $m_{\text{halo,min}}$. This follows because in the fiducial model, the cumulative seed BH mass makes up only $\sim 2\%$ of the redshift zero BH density, so removing some seeds has a negligible effect on the global density. We now turn our attention to the BH scaling relations (Fig. 8c), where we see that the BHs grow on to the observed scaling relations at a higher mass, but that for $M_* \gtrsim 10^{11} M_\odot$ or $\sigma > 100$ km/s the results are almost identical to the fiducial simulation. These are the BHs that are energetically important and we can therefore conclude that results derived from our AGN simulations are insensitive to uncertainties in the minimum halo mass that contains a BH.

Large changes in the mass of the seed BHs (*L050N256HISEED*, *L050N256LOSEED*) can lead to more significant changes in the global properties of the simulation. If the initial seed mass is lowered by a factor of ten then by redshift zero the global BH density is slightly greater than in the fiducial case (Fig. 7c). This occurs because initially smaller BHs take longer to grow onto the BH scaling relations both because they need to grow more and because they grow more slowly (see Fig. 1). As a result of this the galaxy potential well is deeper by the time that the BH begins to heat gas, and so it requires more energy input for the BH to stop its own growth. Because it takes longer for AGN feedback to become effective, the global SFR is higher (Fig. 6c). The same argument can be made in reverse for high seed masses and explains why increasing the BH seed mass slightly decreases the global star formation rate (Fig. 6c). We can draw the same conclusions from examining the SSFR of individual objects (Fig. 9c). Changing the seed mass has virtually no effect on the SFR of the most massive objects, and only affects haloes near the threshold mass at which AGN feedback begins to become important.

The cumulative amount of seed BHs in the simulation *L050N256HISEED* is within a factor of four of the redshift zero black hole density. Although this does not violate our constraint that the total mass in seed BHs should be less than the observed redshift zero value, it is barely satisfied, and leaves very little room for AGN in our simulations to grow. Additionally a large value for the initial seed mass means that we place seed BHs initially *above* the BH scal-

ing relations (Fig. 8c). Nevertheless they still grow onto the same scaling relations.

We note that all our global results are a very weak function of the seed mass. For example, changing the seed mass by a factor of 100 changes the global SFR by no more than a factor 2.5. Other uncertainties, particularly those introduced by our lack of knowledge about the way in which BHs accrete, lead us to conclude that the specifics of the seed model are relatively unimportant.

5.2.3 The feedback efficiency

The efficiency with which a BH's radiated energy is coupled to the ambient gas, ϵ_f , is treated as a free parameter in our simulations. We show in this section that this parameter controls the normalization of the total mass in BHs and of the BH scaling relations (see also Di Matteo et al. 2005). In our simulations ϵ_f was tuned to match the $z = 0$ $m_{\text{BH}} - m_{\text{halo}}$ relation and the redshift zero cosmic black hole density. A value of $\epsilon_f = 0.15$ was found to work well.

Changing ϵ_f from its fiducial value has no discernible effect on the global star formation rate (Fig. 6d), or on the SSFRs of individual objects (Fig. 9d), but the total redshift zero BH density is inversely proportional to the feedback efficiency (Fig. 7d). Most strikingly, simulations *L050N256VHIEPS*, *L050N256HIEPS*, *L050N256LOEPS*, and *L050N256VLOEPS* have values of ϵ_f that differ by factors of 4, 2, 1/2, and 1/4 from the fiducial run, and the ratio of their $z = 0$ BH densities to that of the fiducial simulation are 0.24, 0.53, 1.93 and 4.03 respectively. The fact that the final mass of BHs is directly proportional to $1/\epsilon_f$ implies that in our models any given BH grows until it has injected a specific amount of energy per unit halo mass, at which point it is able to reduce its local density and to effectively self-regulate its growth. As demonstrated in Booth & Schaye (2009) this remarkable result agrees qualitatively with the ideas presented in e.g. Fabian (1999) and Silk & Rees (1998), where BHs grow until they can expel gas from the galaxy, at which point they enter a quiescent phase.

The redshift zero global BH density (Fig. 7d) and the normalization of the BH scaling relations (Fig. 8d) are both directly proportional to $1/\epsilon_f$, and so we can use these observations to constrain the value of ϵ_f that allows our model to be consistent with redshift zero observations. We employ a value of $\epsilon_f = 0.15$ in the present study, but note that we will show elsewhere that the parameters of the AGN model must be tuned in conjunction with the SN feedback prescription.

5.2.4 The heating mechanism

The resolution of cosmological simulations is too poor to resolve the scales on which AGN inject energy into the ISM and as such we are forced to make some assumptions. It is therefore important to verify that the results obtained from our simulations do not depend strongly on the implementation of the energy coupling mechanism.

Two parameters control how energy is distributed from the AGN to its surroundings: the minimum temperature increase and the number of neighbouring SPH particles to heat ($\Delta T_{\text{min}} = 10^8$ K and $n_{\text{heat}} = 1$). The fiducial value of the minimum temperature increase was constrained by

two competing effects. Firstly, if ΔT_{\min} is too low, the cooling time of heated gas will be so short that the gas will be able to radiate away its energy before having a dynamical effect. On the other hand, if ΔT_{\min} is set too high, then the amount of energy needed to perform a heating event will be so high that the numerically determined time between heating events exceeds the Salpeter time-scale, making it impossible for the BH to regulate its growth. We found that $\Delta T_{\min} = 10^8$ K provides a good compromise between these two effects. Similarly, to minimize the numerically controlled duty cycle we set $n_{\text{heat}} = 1$ in our fiducial models. Here we assess the impact of distributing feedback energy in different ways.

If we change either the temperature to which gas is heated from 10^8 K to 10^7 K (*L050N256T7*) or the number of black hole neighbours affected by each feedback event from 1 to 10 (*L050N256HINHEAT*), we see small changes in the cosmic star formation history (Fig. 6e) and in the cosmic BH density (Fig. 7e). We note, however, that the results are relatively insensitive to these parameters, and that changing the value of either ΔT_{\min} or n_{heat} by an order of magnitude affects both BH properties and SFRs by only ~ 0.3 dex. We thus conclude that as long as the feedback efficiency (ϵ_f) is calibrated such that the redshift zero black hole relations are satisfied, and that the minimum heating temperature is sufficient for feedback to be effective, our other results are robust to the precise way in which this energy is coupled to the ISM.

5.2.5 The accretion model

Because numerical simulations cannot resolve the properties of the multi-phase ISM, we can justify the use of high values for the multiplicative factor, α , in the Bondi-Hoyle accretion rate (see Eq. 1), at least for high density gas (Sec. 4). This provides a motivation for the constant- α accretion model – similar to those previously published – where BHs accrete with a very high efficiency. In this paper we have introduced a new class of models that treat accretion of low-density gas differently. By noting that the ISM will not contain a cold ($T \ll 10^4$ K) phase at low pressures and that we are also able to resolve Bondi-Hoyle accretion onto BHs with masses greater than the resolution limit of our simulation if we resolve the Jeans mass, we argue that α must asymptote to unity in low density environments. We then parametrize our ignorance about the state of the multiphase ISM, and the precise mechanism by which AGN accrete by introducing a parameter, β , that describes a power-law dependence of the accretion rate on the local gas density (Eq. 4).

The growth of a black hole depends upon the accretion model used. In the constant- α model (Bondi-Hoyle with $\alpha_0 = 100$) the growth is Eddington limited unless the gas in the immediate surroundings of the BH has a density that is much lower than typical of the ISM, e.g. as a result of feedback from the BH. In the constant- β models, however, much larger densities are required for the accretion rate to become Eddington limited. Efficient growth is only possible if the BH’s local density is enhanced by dynamical processes. BHs can only decrease their accretion rate (and hence regulate their own growth) when densities are low enough that accretion rates are no longer Eddington limited. The density at which BH accretion rates become Eddington limited

depends on the accretion model (Fig. 2). In the constant- α model with $\alpha_0 = 100$ BHs self-regulate at densities below the density at which a multi-phase medium is expected to form (Fig. 2), this has a large effect on the physical properties of the galaxy and because the simulations resolve Bondi-Hoyle accretion in this regime it invalidates the assumptions used to justify the use of $\alpha_0 = 100$ in the first place.

We now consider how changes in the accretion model affect the properties of the simulated galaxy population. Increasing β from 2 to 4 (simulation *L050N256B4*) depresses the global star formation rate somewhat (Fig. 6f) because the β parameter controls the gas density at which the accretion rate for a given BH mass becomes Eddington limited (Fig. 2). Hence, for a given value of β there is a critical value of the local gas density above which a BH can ‘switch on’ and begin to grow rapidly. For larger values of β this occurs at a lower density, and hence in smaller haloes. This manifests itself in the BH scaling relations by changing the minimum galaxy mass at which the BHs grow onto the observed scaling relations. A lower value of β therefore increases the global star formation rate by allowing BHs to grow only in more massive haloes. Increasing β above 4 does not have a large effect on any of our results, as for any large value of β , the BH accretion model behaves in such a way as to be Eddington limited in star-forming gas (Fig. 2), and the difference in behaviour between a $\beta = 4$ model and a $\beta = \infty$ model is very small. Any physical process that is strongly dependent on the local density is affected by numerical resolution, because higher resolution simulations allow the formation of higher density regions. For this reason we caution that the stellar mass at which BHs grow onto the observed relation is affected by numerical resolution, and so the value of β may need to be tuned to different values for simulations with mass resolutions significantly different to those presented here.

A comparison of the effect of different β models on the SSFR of haloes (Fig. 9f) supports this picture. The stellar mass above which the behaviour of each AGN model diverges from the behaviour of the simulation without AGN depends upon the value of β .

In the constant- α model with $\alpha_0 = 100$ (*L050N256A100B0*) BHs grow in an Eddington limited manner from their birth, and as such suppress star formation in all haloes that contain a BH. This is visible in Fig. 9f, in which the constant- α simulation deviates from the simulation without AGN in haloes with a low stellar mass. The constant- α simulations efficiently suppress star formation in every halo that contains a BH and as such the integrated SFR is more than an order of magnitude lower than in the other simulations. The same effect is present in the large simulation volume, but is less pronounced because seed mass BHs are placed only into larger haloes, where both accretion models are capable of suppressing SF. This result implies that in order for a simulation that employs a constant- α accretion model to reproduce the observed break in galaxy properties at $\log(M_*) \sim 10.5$ (e.g. Kauffmann et al. 2003), the resolution must be tuned such that BH seeds are placed into haloes of the correct size⁹.

⁹ Because the accretion rate also depends on the assumed effective EOS, this may not be true for all constant- α models used in

Considering now reducing the value of α_0 in the constant- α models from 100 to 1 (*L050N256A100B0* compared to *L050N256B0*; a constant- β model with $\beta = 0$ is equivalent to a constant- α model with $\alpha_0 = 1$), equivalent to removing the numerical ‘fudge factor’ from the BH accretion rates, we see that BHs are unable to grow in all but the very most massive haloes (Fig. 8f), and so the halo SSFRs are virtually the same as for the simulation without AGN feedback in all haloes up to a stellar mass of $10^{12} M_\odot$ (Fig. 9f). This, in turn, means that the global SFR density in the $\alpha_0 = 1$ simulation is very similar to that in the simulation run without AGN (Fig. 6f). The global BH density at redshift zero is actually higher than that in the fiducial simulation (Fig. 7f). This occurs because the BHs that do grow in the $\alpha_0 = 1$ simulation grow very late, and so find themselves in a deeper potential well. In order to self-regulate they then need to output more energy and hence grow even more than in the other simulations. The global BH density is therefore by itself not a good indicator of how efficiently AGN are able to suppress star formation.

We now consider increasing α_0 by an order of magnitude relative to the usual value (*L050N256A1000B0* compared to *L050N256A100B0*). We already know that the density below which BHs can self regulate depends strongly on the value of α_0 (Fig. 2), and it follows that the value of α_0 will have a strong effect on the physical conditions in the centres of haloes. In the case of $\alpha_0 = 1000$ the global BH density is similar to the $\alpha_0 = 100$ case (Fig. 7f), whereas the global SFR and galaxy SSFRs are much lower than in any other simulation (Fig. 6f and Fig. 9f), and the $m_{\text{BH}} - m_{\text{stellar}}$ relation is shifted significantly to the left as the BHs effectively shut down star formation in all haloes. However, the $m_{\text{BH}} - \sigma$ relation is not as strongly affected by the very effective AGN feedback. This is likely due to the fact that the stellar velocity dispersion tracks the depth of the galaxy potential well, which contains a large contribution from dark matter, whereas the galaxy stellar mass is sensitive to the details of the feedback processes operating inside the galaxy. We see that changing the value of the free parameter α_0 can have profound effects on the simulated galaxy population, even if the evolution in the global mass density of BHs is barely affected by the parameter change.

We conclude this section by noting that predictions from AGN feedback models of this type are sensitive to the accretion model that is used. More generally, it is not clear that the Bondi-Hoyle rate is the correct accretion rate to use in the case of a BH accreting from a hot halo (Krumholz et al. 2006). We find that a different parametrization of the accretion rate leads to profound differences in the star formation histories and speed of BH growth and therefore caution the reader that the AGN accretion mechanism represents a significant source of uncertainty in all our results.

the literature. In the models of S05, which employ an EOS that is initially stiffer than our $\gamma_{\text{eff}} = 4/3$, the BH growth time has a local minimum at $n_{\text{H}} = n_{\text{H}}^*$ which suppresses AGN growth relative to our constant- α model (Springel, private communication).

6 DISCUSSION AND CONCLUSIONS

We have presented and tested a method to incorporate SMBHs into cosmological, smoothed particle hydrodynamics simulations. The method, which is a substantially modified version of the one introduced by S05, self-consistently describes the mass growth of BHs and feedback from AGN. Here we consider growth through mergers with other BHs as well as through accretion of gas. The AGN feedback in our model is thermal and local to the BH.

Although we also use the SPH code GADGET III, our code differs from that of S05 in many ways, including the use of different models for star formation, feedback from SN, radiative cooling and stellar evolution. Particularly relevant for AGN feedback is the fact that, contrary to S05, we do not make use of a subgrid model to describe the different phases of the ISM. Following S05, we make use of subgrid BHs to allow BH masses to be small compared with the masses of the particles containing the BHs. We note, however, that while this approach allows one to significantly extend the range of BH masses in the simulation, the accretion radius will only be resolved if the BH mass exceeds the local Jeans mass. Unfortunately, this is generally not the case if the BH mass is small compared with the particle mass.

The AGN model is specified by seven main parameters (Table 1). Two parameters describe the BH seed generation mechanism: the BH seed mass, m_{seed} , and the halo mass into which seed BHs are placed, $m_{\text{halo,min}}$. Two parameters describe the amount of energy that is coupled back to the ISM per unit accreted mass: ϵ_r , the radiative efficiency of a BH accretion disk, is the fraction of the rest mass energy accreted by the BH that is radiated by the AGN and ϵ_f is the fraction of the radiated energy that is coupled thermally to the ISM. For a given BH accretion rate, the rate at which energy is injected into the ISM depends only on the product $\epsilon_r \epsilon_f$. However, we do need to specify the radiative efficiency ϵ_r since the mass growth of the BH is proportional to $(1 - \epsilon_r)$. A further two parameters control the numerical implementation of the injection of energy into the ISM by AGN: the number of neighbouring gas particles heated by each BH heating event, n_{heat} , and the minimum amount by which their temperature is increased, ΔT_{min} . Because we let BHs store feedback energy until they have saved enough to heat n_{heat} particles by ΔT_{min} degrees Kelvin, these last two parameters together determine the AGN duty cycle for a fixed accretion rate. Finally, we require one additional parameter that controls how BHs accrete gas, and we describe two different models for this process.

The gas accretion rate is assumed to scale as the Bondi-Hoyle accretion rate, evaluated at the location of the BH and on the scales resolved by the simulation. We do not, however, allow the accretion rate to exceed the Eddington rate. The Bondi-Hoyle accretion rate predicted by the simulation will underestimate the true rate if the density is underestimated or if the temperature is overestimated. A lack of numerical resolution may result in an underestimate of the gas density, which motivated S05 to multiply the Bondi-Hoyle rate predicted by the simulation by a constant factor $\alpha_0 = 100$. We call models of this type constant- α models. We noted that cosmological simulations lack not only the resolution, but also the physics to model the cold ISM phase. For example, our simulations use a polytropic effective equation of

state for densities at which the gas is expected to be multiphase. Hence, they will miss the cold component for which the Bondi-Hoyle accretion rate would be highest. This will lead us to strongly underestimate the Bondi-Hoyle rate in high density gas.

Although cosmological simulations cannot yet resolve cold, interstellar gas, many do resolve the Jeans scales at densities low enough for the ambient ultraviolet radiation to suppress cooling below 10^4 K. Specifically, any simulation that resolves the Jeans scales in the gas surrounding a BH particle, will also resolve the Bondi-Hoyle radius if the BH mass exceeds the local Jeans mass. Hence, at sufficiently low densities the Bondi-Hoyle accretion rate is modeled correctly and multiplying it by $\alpha_0 = 100$ would result in a large overestimate of the accretion rate.

We therefore introduced a second class of models in which the Bondi-Hoyle accretion rate is multiplied by a factor $(n_{\text{H}}/n_{\text{H}}^*)^\beta$ for densities $n_{\text{H}} > n_{\text{H}}^*$, where n_{H}^* is the density above which the gas is expected to be multiphase (we take $n_{\text{H}}^* = 0.1 \text{ cm}^{-3}$). We refer to this class of models as constant- β models. Note that both constant- α and constant- β models use a single free parameter. Because we have changed the density-dependence of the accretion rate, we cannot claim to be simulating Bondi-Hoyle accretion, even though the changes are motivated by the Bondi-Hoyle formula and even though we do retain the Bondi-Hoyle scaling with the BH mass. We argued, however, that this is also true for constant- α models because the use of values $\alpha_0 \gg 1$ implies that the densities and temperatures predicted by the simulations are greatly in error.

The parameters α_0 and β , used in the constant- α and constant- β models respectively, control the ambient gas density at which the BH accretion rate becomes Eddington limited (Fig. 2). Because the maximum densities sampled by the simulation increase with halo mass (both because more massive haloes are resolved with more particles and because the central pressure increases with the depth of the potential), these parameters effectively set the halo mass above which BHs can grow efficiently. We set $\beta = 2$, which we find results in efficient BH growth in haloes with stellar masses $\gtrsim 10^{10.5} M_\odot$ in these simulations. Using a constant- α prescription with $\alpha_0 = 100$ implies that, in the absence of AGN feedback, the accretion rate is essentially always Eddington limited. Because the accretion is efficient even at relatively low gas densities, AGN feedback is in that case important in all haloes that exceed $m_{\text{halo,min}}$. For this class of models the halo mass above which AGN can suppress star formation is thus in effect a free parameter ($m_{\text{halo,min}}$). For BHs with masses greater than $10^6 M_\odot$ self-regulation can only occur at densities orders of magnitude below the star formation threshold (Fig. 2). In this regime we resolve Bondi-Hoyle accretion, invalidating the assumption used to justify large values of α in the first place. Constant- α models therefore underestimate the gas density required for self-regulation and will thus overestimate the suppression of the star formation rate.

Having chosen a prescription for gas accretion, we then derive values for the other model parameters. Because each BH stores its feedback energy until it suffices to heat n_{heat} neighbours by ΔT_{min} , we are faced with a numerically determined duty cycle (for a given accretion rate). In order for the BH to be able to regulate its growth, we require the time

between heating events, $\Delta t_{\text{heat}} \propto n_{\text{heat}} \Delta T_{\text{min}}$, to be as small as possible and certainly smaller than the Salpeter time if the accretion is Eddington limited. We use $\Delta T_{\text{min}} = 10^8$ K, which ensures the temperature of the heated gas is high enough that the injected thermal energy is not just radiated away, and $n_{\text{heat}} = 1$, which minimizes Δt_{heat} . Because Δt_{heat} decreases with the ratio of the mass of the BH to that of the heated gas particle, the requirement that Δt_{heat} is smaller than the Salpeter time for Eddington-limited accretion implies that the (subgrid) BH mass must exceed 0.1 per cent of the gas particle mass (Fig. 3). Hence, we set $m_{\text{seed}} = 10^{-3} m_{\text{g}}$. We set $m_{\text{halo,min}} = 100 m_{\text{DM}}$ in order to ensure that seed BHs are placed only into well defined haloes. These parameter values will obviously need to be increased if they result in seed and/or minimum halo masses that are lower than expected physically, as may be the case for simulations that use a much higher resolution than is used here.

We assume the standard value $\epsilon_r = 0.1$ for the radiative efficiency and tune ϵ_f to match the redshift zero $m_{\text{BH}} - m_{\text{halo}}$ relation and cosmic BH density. A value of $\epsilon_f = 0.15$ was found to provide a good match to the observations.

Having specified the AGN model, we then analysed the results from a large suite of cosmological simulations chosen to investigate the sensitivity of the predictions on the model parameters. For this purpose we compared the predictions for the cosmic SF history, the cosmic BH density, the redshift zero BH scaling relations (both the $M_{\text{BH}} - M_*$ and the $M_{\text{BH}} - \sigma$ relations), and the redshift zero galaxy specific star formation rates (SSFRs).

We demonstrated that the fiducial model provides good agreement with both the observed mass density in BHs (Fig. 7) and the BH scaling relations (Fig. 8), and that the inclusion of AGN feedback in the simulations effectively suppresses star formation in galaxies with stellar masses greater than $> 10^{10.5} M_{\text{dot}}$ (Fig. 9). We will discuss the comparison between the simulated global SFR density and observations elsewhere, but for now we note that the SN feedback parameters of our models were tuned such that a simulation without AGN feedback has a peak SFR density that is in good agreement with observations. As such, adding an extra source of feedback energy inevitably results in an underestimate of the SFR density. In order to achieve a good match with observations the properties of the SN model must be tuned in conjunction with those of the AGN model.

However, the focus of our study was not to match observations, but to explore the dependence of the results on the parameters of the model. Our main conclusions are summarised below:

- Regardless of whether BH seeds are initially placed above or below the BH scaling relations, they grow onto the same relations.

- Because the global BH density is dominated by massive BHs and because AGN feedback is only important in high-mass haloes, uncertainties in the seed model employed do not lead to significant changes to the global properties of our simulations. Changing the initial seed mass by two orders of magnitude changes the global star formation rate by only a factor of 2.5. The assumed seed generation model can, however, affect galaxy properties at around the galaxy mass where AGN first begin to become energetically important.

At higher masses galaxy properties are largely insensitive to the initial distribution of BH seeds.

- As discussed more comprehensively in Booth & Schaye (2009), the normalization of both the global BH density and the BH scaling relations is nearly exactly inversely proportional to the AGN feedback efficiency, $\epsilon_r \epsilon_f$. Most strikingly, changing the efficiency by a factor 16 does not give rise to any discernible changes in the global SF history. These results imply that the total amount of thermal energy injected by AGN is conserved when the feedback efficiency is changed. These results can be explained if BHs grow until they have generated enough energy to regulate the accretion rate and if the required amount of energy depends on the depth of the potential well on scales that are larger than the radius on which the BH dominates.

- Changing the way in which the thermal energy from the AGN is distributed in the gas surrounding the BH has little effect on our results, as long as the gas is heated to a temperature that is high enough for its cooling time to become long. Hence, thermal feedback can be efficient in cosmological simulations that do not resolve the multiphase ISM.

- Cosmological simulations currently underestimate the Bondi-Hoyle accretion rate in dense gas because they lack both the resolution and the physics to model the dense, cold phase of the ISM. It is therefore necessary to increase the predicted accretion rate by a fudge factor, either by explicitly multiplying the accretion rate by a numerical correction factor or by employing a subgrid model for the unresolved gas physics to artificially boost accretion rates in star-forming gas. Using a multiplicative factor that asymptotes to unity in the regime where the simulation is able to model the relevant physics (our constant- β model) gives different results from using a high factor throughout (the constant- α model) as has been used in most previous work. In general, the density above which BHs are able to accrete efficiently depends upon the accretion model used (Fig. 1). Because higher mass haloes contain higher density gas, the accretion model determines the halo mass above which AGN feedback becomes effective. Until the simulations are able to resolve Bondi-Hoyle accretion in a multiphase ISM, the predictions of the models will remain subject to significant uncertainty.

- The $m_{\text{BH}} - \sigma$ relation is more robust than the $m_{\text{BH}} - M_*$ relation to changes in the model parameters (Fig. 8), and so provides a test of the numerical model that is less affected by uncertainties in numerical parameters than the Magorrian relation. This is likely due to the fact that the stellar velocity dispersion tracks the depth of the galaxy potential well, which contains a large contribution from dark matter, whereas the galaxy stellar mass is sensitive to the details of the feedback processes operating inside of the galaxy.

In summary, we have presented and tested a new model for the self-consistent growth of BHs and feedback from AGN in cosmological simulations. In a future work we will discuss the interaction between AGN feedback and other physical processes, and show that the results obtained from an AGN model depend also on other processes such as SN feedback and stellar mass loss.

ACKNOWLEDGMENTS

We are very grateful to Volker Springel for generously providing us with a copy of his code. We would also like to thank him as well as Richard Bower, Ian McCarthy and the members of the OWLS collaboration for useful discussions. The simulations presented here were run on the Cosmology Machine at the Institute for Computational Cosmology in Durham as part of the Virgo Consortium research programme, on Stella, the LOFAR BlueGene/L system in Groningen, and on Huygens, the Dutch national supercomputer. This work was supported by Marie Curie Excellence Grant MEXT-CT-2004-014112 and by an NWO Vidi grant.

REFERENCES

- Aller M. C., Richstone D., 2007, 665, 120
 Arav N., Korista K. T., de Kool M., 2002, ApJ, 566, 699
 Arav N., Moe M., Costantini E., Korista K. T., Benn C., Ellison S., 2008, ApJ, 681, 954
 Barnes J. E., Hernquist L. E., 1991, ApJ, 370, L65
 Barnes J. E., Hernquist L. E., 1996, ApJ, 471, 115
 Baugh C. M., 2006, Reports of Progress in Physics, 69, 3101
 Benson A. J., Bower R. G., Frenk C. S., Lacey C. G., Baugh C. M., Cole S., 2003, MNRAS, 599, 38
 Begelman M., Rees M. J., 1978, MNRAS, 185, 847
 Begelman M., Volonteri M., Rees M. J., 2006, MNRAS, 370, 289
 Bhattacharya S., di Matteo T., Kosowsky A., MNRAS, 389, 34
 Bondi H., Hoyle F., 1944, MNRAS, 104, 273
 Booth C. M., Schaye J., astro-ph/????????
 Bower R. G., Benson A. J., Malbon R., Helly J. C., Frenk C. S., Baugh C. M., Cole S., Lacey C. G., 2006, MNRAS, 370, 645
 Boyle B. J., Terlevich R. J., 1998, MNRAS, 293, L49
 Bromm V., Loeb A., 2003, ApJ, 596, 34
 Bruzual G., Charlot S., 2003, MNRAS, 344, 1000
 Buff J., McCray R., 1974, ApJ, 189, 147
 Callegari S., Mayer L., Kazantzidis S., Colpi M., Governato F., Quinn T., Wadsley J., 2008, astro-ph/0811.0615
 Cao X., Li F., 2008, MNRAS, 390, 561
 Cattaneo A., 2001, MNRAS, 324, 128
 Chelouche D., 2008, astro-ph/0812.3621
 Ciotti L., Ostriker J. P., 2001, ApJ, 551, 131
 Colberg J. M., di Matteo T., 2008, MNRAS, 387, 1163
 Cowie L. L., Ostriker J. P., Stark A. A., 1978, ApJ, 226, 1041
 Croft R. A. C., Di Matteo T., Springel V., Hernquist L., 2008, astro-ph/0803.4003
 Croton D. J., 2006, MNRAS, 365, 11
 Dekel A., Silk J., 1986, ApJ, 303, 39
 Dalla Vecchia C., Schaye J., 2008, MNRAS, 387, 1431
 Davis M., Efstathiou G., Frenk C. S., White S. D. M., 1985, ApJ, 292, 371
 Dijkstra M., Haiman Z., Mesinger A., Wyithe S., 2008, astro-ph/0810.0014
 Di Matteo T., Springel V., Hernquist L., 2005, Nature, 433, 604
 Di Matteo T., Colberg J., Springel V., Hernquist L., 2008, ApJ, 676, 33

- Diemand J., Kuhlen M., Madau P., 2007, *ApJ*, 667, 859
- Dolag K., Borgani S., Murante G., Springel V., 2008, *astro-ph/0808.3401*
- Edgar R., 2004, *NewAR*, 48, 843
- Efstathiou G., Rees M. J., 1998, *MNRAS*, 230, 5
- Elvis M., Risaliti G., Zamorani G., 2002, *ApJL*, 565, L75
- Fabian A. C., 1999, *MNRAS*, 308, L39
- Fabbiano G., 2006, *ARA&A*, 44, 323
- Ferland G. J., Korista K. T., Verner D. A., Ferguson J. W., Kingdon J. B., Verner E. M., 1998, *PASP*, 110, 761
- Feoli A., Mele D., 2005, *International Journal of Modern Physics D*, 14, 1861
- Ferrarese L., Merritt D., 2000, *ApJL*, 539, L9
- Ferrarese L., 2002, *ApJ*, 578, 90
- Gebhardt K. et al., 2000, *ApJ*, 539, L13
- Gingold, R. A., & Monaghan, J. J. 1977, *MNRAS*, 181, 375
- Graham A. W., Driver S. P., 2007, *ApJ*, 666, 77
- Graham A. W., Driver S. P., 2007, *MNRAS*, 380, L15
- Graham A. W., 2008, *ApJ*, 680, 143
- Granato G. L., De Zotti G., Silva L., Bressan A., Danese L., 2004, *ApJ*, 600, 580
- Greene J., Ho L. C., Barth A. J., 2008, *astro-ph/08101972*
- Haardt F., Madau P., 2001, in Neumann D. M., Tran J. T. V., eds, *Clusters of Galaxies and the High Redshift Universe Observed in X-rays Modelling the UV/X-ray cosmic background with CUBA*
- Haehnelt M. G., Rees M. J., 1993, *MNRAS*, 263, 168
- Hopkins P. F., Hernquist L., Cox T. J., Di Matteo T., Robertson B., Springel V., 2006, *ApJS*, 163, 1
- Hopkins P. F., Hernquist L., Cox T. J., Robertson B., 2007, *ApJ*, 669, 67
- Hopkins P. F., Hernquist L., Cox T. J., Keres D., Stijn W., *astro-ph/0807.2868*
- Hoyle F., Lyttleton R. A., 1939, *Proc. Cambridge Philos. Soc.*, 35, 405
- Haring N., Rix H. W., 2004, *ApJL*, 604, 89
- Islam R. R. Tayloe J. E., Silk J., 2003, *MNRAS*, 340, 647
- Johansson P. H., Naab T., Burkert A., 2009, *ApJ*, 690, 802
- Kapferer W., Knapp A., Schindler S., Kimeswenger S., van Kampen E., 2005, *AAP*, 438, 87
- Katz N., Weinberg D. H., Hernquist L., 1996, *ApJS*, 105, 19
- Kauffmann G., Haehnelt M., 2000, *MNRAS*, 311, 576
- Kauffmann G. et al., 2003, *MNRAS*, 346, 1055
- Kauffmann G., Heckman T., *astro-ph/0812.1224*
- Kennicutt R. C., 1998, *ApJ*, 498, 541
- Khalatyan A., Cattaneo A., Schramm M., Gottloeber S., 2008, *astro-ph*
- Komatsu E. et al., 2008, *astro-ph/0803.0547*
- Kormendy J., Richstone D., 1995, *ARA&A*, 33, 581
- Krumholz M. R., McKee C. F., Klein R. I., *ApJ*, 638, 369
- Lagos C. D. P., Cora S. A., Padilla N. D., 2008, *MNRAS*, 388, 587
- Laor A., Fiore F., Elvis M., Wilkes B. J., 1997, *ApJ*, 477, 93
- Laor A., 2001, *ApJ*, 553, 677
- Loeb A., Rasio F. A., 1994, *ApJ*, 432, 52
- Lucy, L. B., 1977, *AJ*, 82, 1013
- Lynden-Bell D., 1969, *Nature*, 223, 690
- Madau P., Ferguson H. C., Dickinson M. E., Giavalisco M., Steidel C. C., Fruchter A., 1996, *MNRAS*, 283, 1388
- Madau P., Rees M. J., 2001, *ApJ*, 551, L27
- Magorrian J. et al., 1998, *AJ*, 115, 2285
- Makino J., Funato Y., 2004, *ApJ*, 602, 93
- Marconi A., Hunt L. K., 2003, *ApJL*, 589, L21
- Marconi A. et al., 2004, *MNRAS*, 351, 169
- Merritt D., Ferrarrese L., 2001, *ApJ*, 547, 140
- Martinez-Sansigre A., Taylor A. M., 2008, *astro-ph/0810.3920*
- McLure R. J., Dunlop J. s., 2002, *MNRAS*, 331, 795
- Micic M., Holley-Bockelmann K., Sigurdsson S., Abel T., 2007, *MNRAS*, 380, 1533
- Mihos J. C., Hernquist L., 1994, *ApJ*, 425, L13
- Mihos J. C., Hernquist L., 1996, *ApJ*, 464, 641
- Monaghan J. J., 1992, *ARA&A*, 30, 543
- Murray N., Quataert E., Thompson T. A., 2005, *ApJ*, 618, 569
- Okamoto T., Nemmen R. S., Bower R. G., 2008, *MNRAS*, 385, 161
- Pelupessy F. I., Di Matteo T., Ciardi B., 2007, *ApJ*, 665, 107
- Pounds K. A., King A. R., Page K. L., O'Brien P. T., 2003, *MNRAS*, 346, 1025
- Reed D. S., Bower R., Frenk C. S., Jenkins A., 2006, *MNRAS*, 374, 2
- Robertson B., Hernquist L., Cox T. J., Di Matteo T., Hopkins P. F., Martini P., Springel V., 2006, *ApJ*, 641, 90
- Salpeter E., 1964, *ApJ*, 140, 796
- Schneider R., Ferrara A., Natarajan P., Omukai K., 2002, *ApJ*, 571, 30
- Schaye J., 2004, *ApJ*, 609, 667
- Schaye J., Dalla Vecchia C., 2008, *MNRAS*, 383, 1210
- Shakura N. I., Syunyaev R. A., 1973, *AAP*, 24, 337
- Shankar F., Salucci P., Granato G. L., De Zotti G., Danese L., 2004, *MNRAS*, 354, 1020
- Silk J., Rees M. J., 1998, *AAP*, 3 31, L1
- Sijacki D., Springel V., di Matteo T., Hernquist L., 2007, *MNRAS*, 380, 877
- Spergel D. N., 2007, *ApJS*, 170, 377
- Springel V., Yoshida N., White S. D. M., 2001, *NewA*, 6, 79
- Springel V., White S. D. M., Tormen G., Kauffmann G., 2001, *MNRAS*, 328, 726
- Springel V., Hernquist L., 2003, *MNRAS*, 339, 289 (SH03)
- Springel V., Di Matteo T., Hernquist L., 2005, *MNRAS*, 361, 776 (S05)
- Springel V., 2005, *MNRAS*, 364, 1105
- Thorne K., 1974, *ApJ*, 191, 507
- Toomre A., Toomre J., 1972, *ApJ*, 178, 623
- Tremaine S. et al., 2002, *ApJ*, 574, 740
- Wang J. M., Chen Y. M., Ho L. C. McLure R. J., 2006, *ApJ*, 642, L111
- Wang J. M., Chen Y. M., Hu C., 2006, *ApJ*, 637, L85
- Wiersma R. P. C., Schaye J., Smith B. D., 2009, *MNRAS*, 393, 99
- Wiersma R. P. C., Schaye J., Theuns T., Dalla Vecchia C., Tornatore L., *MNRAS*, submitted, arXiv:0902.1535
- Volonteri M., Natarajan P., *astro-ph/0903.2262*
- Yu Q., Tremaine S., 2002, *MNRAS*, 335, 965
- Yu Q., Lu Y., 2008, *astro-ph/0808.3777*